Evapotranspiration of an abandoned grassland in the Italian Alps: Modeling the impact of shrub encroachment

Journal of Hydrology 635 (2024) 131223

Contents lists available at ScienceDirect

Journal of Hydrology

journal homepage: www.elsevier.com/locate/jhydrol

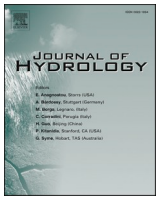

Research papers

Evapotranspiration of an abandoned grassland in the Italian Alps: Modeling the impact of shrub encroachment

Davide Gisolo [a,*], Ivan Bevilacqua [a], Alessio Gentile [a], Justus van Ramshorst [b], Davide L. Patono [c], Claudio Lovisolo [c], Maurizio Previati [a], Davide Canone [a], Stefano Ferraris [a]

[a] Interuniversity Department of Regional and Urban Studies and Planning (DIST), University of Turin and Polytechnic of Turin, 10125 Torino, Italy
[b] Bioclimatology, Faculty of Forest Sciences and Forest Ecology, University of Goettingen, Busgenweg 2, 37077 Goettingen, Germany
[c] Department of Agricultural, Forest and Food Sciences (DISAFA), University of Turin, 10095 Grugliasco, Italy

ARTICLE INFO

Keywords:
Shrub encroachment
Abandoned mountain grassland
Hydrus 1D double vegetation
Actual evapotranspiration modeling

ABSTRACT

This study analyzes the effect of shrub encroachment on actual evapotranspiration (ETa), a still poorly studied phenomenon in the Alps. The effect of shrub encroachment is investigated on an Alpine grassland in Western Italy using both data and a soil hydrological model (Hydrus 1D), which is used to model three different land covers: grassland, shrubland, and a mixture of the two land covers with a novel double vegetation approach recently introduced. Four growing seasons of eddy covariance measurements are used as an approximate reference for the interpretation and consistency of the model outputs. Also, the impact of meteorological inter-annual variability and of different environmental conditions on both modeled and measured evapotranspiration is analyzed. The modeling results show that the model is able to capture the inter-annual variability of ETa. The double vegetation approach suggests that the percentage of total transpiration flux assigned to the shrubland is between 20 and 60 %. Single-vegetation simulations show that shrubs lead to an enhancement of ETa equal to + 27.1 %, +26.0 %, +26.8 %, and + 23.9 % (range 2014–2017) compared to grassland, which could lead to an alteration of the hydrological cycle. Moreover, chambers measurements of shrubs transpiration show a good agreement with the eddy covariance measurement, suggesting that the ecosystem's behavior is already close to a shrubland, which yields an increased ETa if compared to grassland. The evaporative index from the modeled shrubland is higher (range +24–27 %) than the case of a modeled grassland.

Finally, ETa and the evaporative fraction (EF) are in the energy-limited regime in most cases. This result was obtained from the analysis of the relationship between ETa (and EF) and either meteorological variables or soil water content including the simulated one in the 0–100 cm horizon. The following analysis, more focused on micrometeorological variables, namely vapor pressure deficit, net radiation, wind speed, air temperature, and ground heat flux, indicates that ETa is mostly affected by the vapor pressure deficit.

1. Introduction

Actual evapotranspiration (ETa) is a key variable of the hydrological cycle. A well-known issue is related to climate change: it implies global warming, and subsequently an increased water vapor demand, therefore ETa is expected to be altered (Calanca et al., 2006). Depending on the vegetation, meteorological and climatological conditions, the ETa change could result in either an increase in ETa in well-watered environments or in reduced ETa due to less water in the soil, higher air humidity, and vegetation strategies (Ben Hamouda et al., 2021; Condon et al., 2020). More in detail, in a warmer climate, ETa should increase following an increased water vapor demand. However, ETa changes also depend on the water regulation mechanisms of vegetation and the vegetation type (Bonan, 2015; Goulden and Bales, 2014). Also, land cover changes can modify ETa (van den Bergh et al., 2018). Furthermore, the strategy of some plant species could lead to a reduction in ETa (because of the limitation of stomatal conductance, Li et al., 2021a,b). This effect might be partially counteracted by the development of vegetation species that can extract water from deep soil layers. In addition, under drought conditions, ETa is affected by abiotic factors and also by water-use strategies in the vegetation (Leitinger et al., 2015). Abiotic factors might also include topographic features (e.g. Gisolo et al., 2022).

* Corresponding author.
E-mail address: davide.gisolo@unito.it (D. Gisolo).

https://doi.org/10.1016/j.jhydrol.2024.131223
Received 11 October 2023; Received in revised form 28 March 2024; Accepted 30 March 2024
Available online 21 April 2024

List of symbols

EF	Evaporative Fraction, –
ETa	Actual evapotranspiration, mm d^{-1} or mm if cumulative over a specified period
ETa/P	Evaporative index, –
ETo	Potential evapotranspiration, mm d^{-1} or mm if cumulative over a specified period
ETa_{Obs}	Actual evapotranspiration from eddy covariance, mm d^{-1} or mm if cumulative over a specified period
$ETa_{Sim\ grass}$	Modeled actual evapotranspiration from grass, mm d^{-1} or mm if cumulative over a specified period
$ETa_{Simshrub}$	Modeled actual evapotranspiration from shrubs, mm d^{-1} or mm if cumulative over a specified period
$ETa_{Simgrass+shrub}$	Modeled actual evapotranspiration with Hydrus 1D "double vegetation", mm d^{-1} or mm if cumulative over a specified period
G_0	Ground heat flux at the surface, W m^{-2} or MJ m^{-2}
MAE	Mean absolute error (ETa or SWC), mm d^{-1} or m^3 m^{-3}
SWC	Soil water content (acronym), m^3 m^{-3} or mm equivalent (if specified)
θ	Soil water content, m^3 m^{-3} or mm equivalent (if specified)
θ_{Obs}	Measured soil water content at 10, 20 or 40 cm of depth, m^3 m^{-3} or mm equivalent (if specified)
$\theta_{Simgrass}$	Modeled soil water content for grass, m^3 m^{-3} or mm equivalent (if specified)
$\theta_{Simshrub}$	Modeled soil water content for shrubs, m^3 m^{-3} or mm equivalent (if specified)
$\theta_{Simgrass+shrub}$	Modeled soil water content with Hydrus 1D "double vegetation", m^3 m^{-3} or mm equivalent (if specified)
P	Precipitation, mm
R	Pearson correlation coefficient, –
R^2	Coefficient of determination, –
RH	Relative humidity, –
R_n	Net radiation, W m^{-2} or MJ m^{-2}
T_{air}	Air temperature, °C
U	Wind speed, m s
VPD	Vapor pressure deficit, kPa

Particular attention should be devoted to analyzing water-limited environments, characterized by low precipitation input. These environments include arid, semiarid, and subhumid areas, and represent half of the terrestrial land surface (Newman et al., 2006). Water-limited environments can also be found in the Alpine region (e.g. Bertoldi et al., 2014). In this area, the water stress significantly affects the grassland response, but with increasing elevation the limiting variable is energy (Carrer et al., 2019; Della Chiesa et al., 2014). Eddy covariance measurements on a shrub-encroached, water-limited area were performed by Vivoni et al. (2022) to monitor brush management.

Moreover, the topography, land cover and soil characteristics play a key role in soil water content (Bertoldi et al., 2014). The aforementioned alterations of ETa can lead to even more enhanced and unambiguous responses, as in abandoned Alpine grasslands, especially, but not limited to, water-limited grasslands.

Enhanced responses can occur because mountainous areas are very sensitive to environmental changes (Caviezel et al., 2014), and they experience an elevation-dependent effect of global warming (Palazzi et al., 2019). Unambiguous responses can also be observed, because abandoned grasslands are not characterized by human disturbance, such as grazing. Abandoned grasslands experience a natural land cover change due to plant species colonizing the terrain, a process also known as encroachment. The first species that typically colonize such areas are woody plants, and this type of encroachment is documented worldwide (Archer et al., 2017; Maestre et al., 2009). Moreover, according to Schreiner-McGraw et al. (2020), the shrub encroachment is more important than climate change for drylands. Grassland abandonment and shrub encroachment also occur in the Alps (Caviezel et al., 2017; Tasser et al., 2005), where it is additionally affected by the local topography, leading to enhanced colonization along steep slopes (Komac et al., 2011). Land abandonment in the Alps increased by 34 % in the past century (Baur et al., 2007), and shrub (and tree) encroachment might be responsible for around 10 % of the greening observed in the Aosta Valley (Filippa et al., 2019), the area where the experimental site used for the current paper is located.

Recently, several studies have analyzed abandoned grasslands, but they focused mainly on the ecological or eco-hydrological point of view, considering in particular carbon cycle components and Alpine greening. These studies focused on soil carbon dynamics of areas with land abandonment (Meyer et al., 2012); on the carbon balance at several grassland and abandoned grassland sites (Berninger et al., 2015); on the micrometeorology of ecosystem respiration and net ecosystem exchange (Galvagno et al., 2017); on soil chemical properties and soil carbon characteristics (Ding et al., 2020; Hunziker et al., 2017); on satellite measurements of NDVI for studies on encroachment and its effects on the greening phenomenon in the Alps (Filippa et al., 2019).

Few studies have been devoted to analyzing mountain grasslands from a soil, micrometeorological, and hydrological point of view also using modeling tools such as in Della Chiesa et al. (2014), but many of the studied grasslands are not abandoned and the sites are mostly – although not all – homogeneous. The ETa characterization and interannual variability were studied by Gu et al. (2008) on the Tibetan Plateau, whereas ETa drivers on grassland sites in the Alps (and ETa interannual variability) were studied by Wieser et al. (2008) using 12 grassland sites, including a managed grassland site equipped with eddy covariance. In that study, photosynthetically active radiation (strongly related to global radiation) and VPD were identified as the main drivers. More recently, the surface runoff dynamics of managed and unmanaged grasslands was investigated by Leitinger et al. (2010). The soil-vegetation interaction and evapotranspiration estimation of an area encroached by shrubs in the Swiss Alps were studied by Caviezel et al. (2014). The effects of elevation on hydrologically relevant variables were studied by Della Chiesa et al. (2014), where, using the GEOtop-dv model (Rigon et al., 2006; Endrizzi et al., 2013), an elevational dependency of ETa, water use efficiency (WUE) and aboveground biomass was found. Limited ETa, WUE, and aboveground biomass due to water scarcity were found only below an altitude threshold. Leitinger et al. (2015) mainly focused on managed grasslands, but also analyzed soil water content on abandoned land sites, which showed higher ETa than managed areas. The ETa from abandoned land was comparable with pastures and meadows, whereas never cultivated but summer-grazed grasslands were characterized by lower ETa values (Leitinger et al., 2015). An in-depth eco-hydrological analysis of ETa, its drivers, its inter- and intra-annual variability, and of the topography impact on ETa at the field scale was performed by Gisolo et al. (2022) at the same site of the present paper.

Other research on the shrub encroachment has been proposed in the past few years, as discussed in the following. Abandoned Alpine grasslands with *Alnus* shrubs encroachment were characterized by an enhanced ETa if compared to a grazed grassland, especially on days with high vapor pressure deficit (VPD, van den Bergh et al., 2018). However, several other vegetation species regulate transpiration by closing the stomata at variably high VPD and in low water availability conditions (Grossiord et al., 2020). Due to the variable ecosystem responses, the increase in ETa at shrublands is still a debated topic. Recent work by Tang et al. (2018) showed that some shrub species among which

Hippophae rhamnoides are anisohydric, such as grass (Martre et al., 2001). The presence of shrubs also increases the roughness length due to higher vegetation if compared to grass (e.g. Foken, 2008) and, hence, aerodynamic resistance. Also turbulent fluxes are affected, since sensible heat flux is expected to decrease, whereas latent heat flux and, hence, ETa increase (He et al., 2010; Bonfils et al., 2012). Larger changes in ETa components compared to ETa total flux in the case of shrub encroachment processes can be explained by alterations of canopy resistance and the interaction between water use patterns and the ecosystem characteristics (Wang et al., 2018). In another recent study, Li et al. (2021a,b) found, for a type of shrub (*Potentilla fruticosa*), a reduced annual ETa from the shrubland site if compared with the meadow site because of increased bulk surface resistance of the shrubland.

Shrub encroachment, which will likely accelerate in the global warming context (Komac et al., 2013), also modifies the soil water content. Among the below ground properties, recently, Schreiner-McGraw et al. (2020) showed that encroachment is also important for the future evaluation of groundwater. Additionally, shrubs are responsible for the enhancement of slope stability (Caviezel et al., 2014). They also increase the deep soil water uptake and cause a lower water content if compared to grass (Wang et al., 2012). However, according to another recent study, shrub encroachment increases water availability with consequent ETa increase (Wang et al., 2018). Shrubs are capable of increasing fresh carbon in the soil (Hunziker et al., 2017) and their existence results in a lower foliage temperature compared to grass (van den Bergh et al., 2018). Moreover, ecosystem services are altered if shrub encroachment occurs, with a possible collapse of provisioning services (Schirpke et al., 2017).

A comparison of ETa with both hydrological model and observations was proposed by Wegehenkel and Beyrich (2014), who collected eddy covariance data and modeled evapotranspiration over a managed and homogeneous grassland using Hydrus 1D. The simulations provided a good agreement with eddy covariance and soil water content (SWC) data. The reconstruction of soil water content by means of satellite images and of a hydrological model was also tested by Bertoldi et al. (2014) on a mountain grassland site. However, the focus was on the soil water content, and the grassland was not colonized by shrubs. More recently, Bottazzi et al. (2021) applied the GEOframe-Prospero model at several sites around the world. One of the sites used was Torgnon, located in the Western Italian Alps (Aosta Valley). That site is located on an abandoned grassland (but not encroached by shrubs). A rather good agreement was found between modeled and measured data.

Measurements and modeling studies on changes in ETa due to encroachment on abandoned grasslands are still rare, especially in complex terrains with a mixture of grass and shrubs and located in the Western Alps. Such studies can contribute to a better understanding on how these ecosystems work and on how they respond to environmental changes. In particular, these analyses are important in areas such as the internal Alpine regions, which are normally characterized by a low precipitation in the summer or in the hydrological year (in the range 300–500 mm). This problem could be worsened in areas with ephemeral snow cover (as the site analyzed in the present paper) which leads to less soil water infiltration, if compared with sites with seasonal snowpacks (Gentile et al., 2023). In addition, the water availability could decrease because of the reduction of glaciers and of seasonal snow quantity and duration (Carrer et al., 2023). Furthermore, particularly warm growing seasons with long dry periods could lead to major water cycle alterations, which could be worsened, due to ETa enhancement, that would further reduce groundwater recharge (Condon et al., 2020). On the other hand, these effects could be counteracted by very low soil water content (SWC) and by the development of isohydric vegetation (i.e. some shrubs species) instead of anisohydric vegetation.

The current study uses observed (eddy covariance) and simulated actual evapotranspiration (with Hydrus 1D model). The simulations are based on three different land cover types: grassland, shrubland and a combination of the two land covers. One important aim is to model the mixture of vegetation types, simulated using a particular novel set-up of Hydrus 1D, using a double vegetation approach allowed within the modified software. The analysis has the following objectives: 1. Validate the simulations (with single and double vegetation approaches) and determine which of the two simulated land covers (grass versus shrubs) is closer to observations, also considering temporal variability. 2. Quantify the difference in modeled ETa between the two different land covers (grassland versus shrubland), and how this changes temporally. 3. Understand in which environmental conditions the model better simulate the ETa observations (with both the double vegetation and single vegetation approaches). 4. Understand what are the main environmental variables that influence ETa, the differences between simulations (with double vegetation model approach) and observations of ETa, and the differences between simulation runs (using the single vegetation mode, with either grass or shrubs).

Fig. 1. The Cogne site. Shrubs are evident around the eddy covariance station.

2. Materials and methods

2.1. The site

The measurement site is located in Cogne, Valle d'Aosta, Italy (45.615N, 7.3585E, 1730 m a.s.l. Fig. 1). The local growing season typically ranges from June to September. The site is on a 26° (on average) slope which has a south-southeast aspect (169°). The average yearly precipitation was 672 mm for the period 1995–2019, whilst the average precipitation in the growing season (June-September) was 230 mm. The average yearly temperature in the same period was 5.3 °C and the average temperature of the growing season was 12.5 °C. The flux footprint extends for about 80 m around the station (Gisolo et al., 2022). The experimental site is located on an abandoned grassland, and neither grazing nor irrigation have occurred for at least forty years.

The vegetation consists of herbaceous species of the genus *Festuca* with a canopy height of about 0.3 m and shrubs (*Hippophae rhamnoides*, buckthorn bushes, *Lycium*) with a canopy height ranging from 0.8 to 1 m. These shrubs are typical for abandoned grasslands at medium–high altitudes. The maximum soil depth is 1.5 m, and the soil is characterized by a sandy loam texture (73 % sand, 22 % loam and about 5 % of clay) with some gravel. According to the soil map of Aosta Valley (D'Amico et al., 2020), the soil at Cogne, within the station footprint, is divided in two areas, one with Petric/Haplic Calcisol soil and one with Haplic Kastanozem. The measured soil bulk density is $1.40{\cdot}10^{3}$ kg m^{-3}. In situ observations have shown that the snow cover at the site lasts no more than a few days or weeks after each snowfall event (and the snowfalls do not occur after April). The snow depth is rarely beyond 60 cm. Moreover, as illustrated also in Raffelli et al. (2017), the soil at the site is

Table 1
Main hydrological characteristics at the experimental site (Gisolo et al., 2022). The dry spell refers to the period May-September (MJJAS). The ETa/P ratio (evaporative index, Budyko, 1974) refers to growing season (JJAS) evapotranspiration and to precipitation of the hydrological year.

	Dry spell (MJJAS) (days)		RH (JJAS) (%)	*P* (May) (mm)	*P* (JJAS) (mm)	*P* (hydrological year) (mm)	T_{air} (JJAS) (°C)	*ETa/P* (%)
	AVG	MAX	AVG	SUM	SUM	SUM	AVG	
2014	4.2	14	67.1	69.4	263.0	695.6	12.0	52.7
2015	6.6	28	64.0	66.3	317.6	752.6	13.3	46.0
2016	5.5	15	58.6	111.8	179.0	640.4	13.4	38.2
2017	6.1	20	57.4	53.8	182.0	623.6	13.2	36.1

incoherent, and the groundwater recharge does not occur locally, because of water drainage at the soil bottom. The choice of using growing season data is also motivated by isotopic analyses at snow-dominated catchments, which showed that the snowmelt rapidly infiltrates in the soil, and it is likely not used by vegetation (Gentile et al., 2023).

The station is equipped with eddy covariance instrumentation, parallel to the slope, at 2 m above ground (one three-dimensional sonic anemometer, CSAT3, Campbell Scientific, Logan, UT, USA, and one open path infrared gas analyzer, LI-7500A, LI-COR, Lincoln, NE, USA) and non-eddy covariance instruments, including: 1. three soil water content probes (CS616, Campbell Scientific, Logan, UT, USA) at 10 cm (in 2014) and at 20 and 40 cm (from 2015) within the soil profile. 2. Two thermocouples 8 cm deep (TCAV, Campbell Scientific, Logan, UT, USA). 3. One snow depth sensor (SR50AT, Campbell Scientific, Logan, UT, USA). 4. Two 8 cm deep soil heat flux plates (HFP01SC, Hukseflux Thermal Sensors, Delft, The Netherlands). 5. One infrared surface temperature sensor (IRTS-P, Apogee Instruments, Logan, UT, USA). 6. One four-component radiometer parallel to the terrain slope at 2 m (NR01, Hukseflux Thermal Sensors, Delft, The Netherlands) for shortwave, longwave and net radiation. 7. One thermohygrometer (HMP45C, replaced in January 2015 by a HMP155A, Vaisala, Vantaa, Finland). The hourly precipitation data were collected at the Regional Authority (ARPA-VdA) standard site (150 m West of the Cogne station) using a heated rain gauge. More details about the site are provided in Raffelli et al. (2017) and in Gisolo et al. (2022).

2.2. Eddy covariance data processing

The eddy covariance 10 Hz data were processed using the EddyPro 6.2.1 software (LI-COR Biogeosciences, Lincoln, USA). The operations of processing and post-processing are described in detail by Gisolo et al. (2022). The same dataset described in the previous paper is used in the current study aggregated at the half-hourly, hourly, and daily scales.

2.3. Data analysis: Hydrological characteristics of the site

The analyzed data set includes data collected between 2014 and 2017 during the local growing season (June-to-September – JJAS). As illustrated in Gisolo et al. (2022) two wet (2014 and 2015) and two dry (2016 and 2017) growing seasons can be identified (Table 1). Besides, one growing season (2014) is also colder, on average, than the other three (Table 1). The identification of two wet and two dry growing seasons relies on the combination of dry spells (number of consecutive dry days, defined as days with less than 1 mm of precipitation according to Baiamonte et al., 2019), relative humidity (RH), precipitation (P) and the *ETa/P* ratio.

2.4. Modeling actual evapotranspiration with different land covers

2.4.1. Model set-up

The hydrological model Hydrus 1D in the single vegetation mode, version 4.17 (Simunek et al., 2012), is used to model the water balance at the Cogne site for the two different land covers (grassland and shrubland) at the hourly scale. The input data are precipitation and potential evapotranspiration (ETo), calculated using the Penman-Monteith FAO 56 formula with meteorological values measured at the station (Allen et al., 1998).

Table 2
Soil parameters in the HYDRUS 1D model set up before (considering a sandy loam soil type) and after optimization. θ_r: residual soil water content, θ_s: saturation soil water content; α, n, K_s, l: van Genuchten water retention curve parameters.

	θ_r(m^3 m^{-3})	θ_s(m^3 m^{-3})	α(cm^{-1})	*n* (–)	K_s (cm h^{-1})	*l* (–)
Initial guess	0.037	0.387	0.0403	1.553	3.74	0.5
Optimization	0.000	0.426	0.0025	1.733	2.11	0.0

The double vegetation Hydrus 1D model (whose inputs are the same as previously indicated), instead, allows to model up to two vegetation types, each one with its root depth and distribution in the soil and with its own water stress parameters, as illustrated below. The soil column, for both the single vegetation and double vegetation modes, is simulated also using other known characteristics of the site (vegetation, soil texture, bulk density, bedrock depth). A more detailed description of the Cogne site characteristics can be found in Raffelli et al. (2017) and Gisolo et al. (2022). The finite elements mesh divides the soil column into 101 equally distributed nodes (the default set-up of Hydrus was considered acceptable for the purpose of the work) and into eight layers – or horizons (0–10 cm, 10–15 cm, 15–20 cm, 20–30 cm, 30–40 cm, 40–80 cm, 80–100 cm, and 100–150 cm).

The approach of Feddes et al. (1978) for root water uptake stress response function (hence, ETa limitation due to soil water content, or the associated pressure head) is used with some modification.

The new Feddes parameters from Peters et al. (2017) are used for the grassland simulations. The Feddes parameters for olive trees described by Minacapilli et al. (2009) were considered reasonably similar to the shrubs species found at Cogne, therefore these are applied in the shrubland simulations. The aforementioned parameters for grass and shrubs are used also in the double vegetation simulations.

Root depths are assumed, respectively, 30 cm for grass and 150 cm for shrubs. These values are based on surveys at the site and on the study of Turekhanova (1995). Between 0 and 40 cm of soil depth, the measured SWC is used for the initial condition. The initial values of soil moisture at 10 cm (for 2014) and at 20 and 40 cm (from 2015 onwards) are the measured values at the midnight of 1st June for each growing season. The initial value at 10 or 20 cm is valid for the soil profile between 0 and 20 cm. Between 20 and 40 cm, the initial values are set using the measure at 40 cm, where the deepest probe is located. From 40 cm down to 150 cm of depth, the initial profile of SWC is linearly increasing from the measure at 40 cm (always around 0.1 m^3 m^{-3} at the beginning of the season) to 0.15 m^3 m^{-3} (field capacity) at the bottom. The boundary condition at the surface is determined by the atmospheric conditions, whereas at the bottom of the soil column it is set to free drainage.

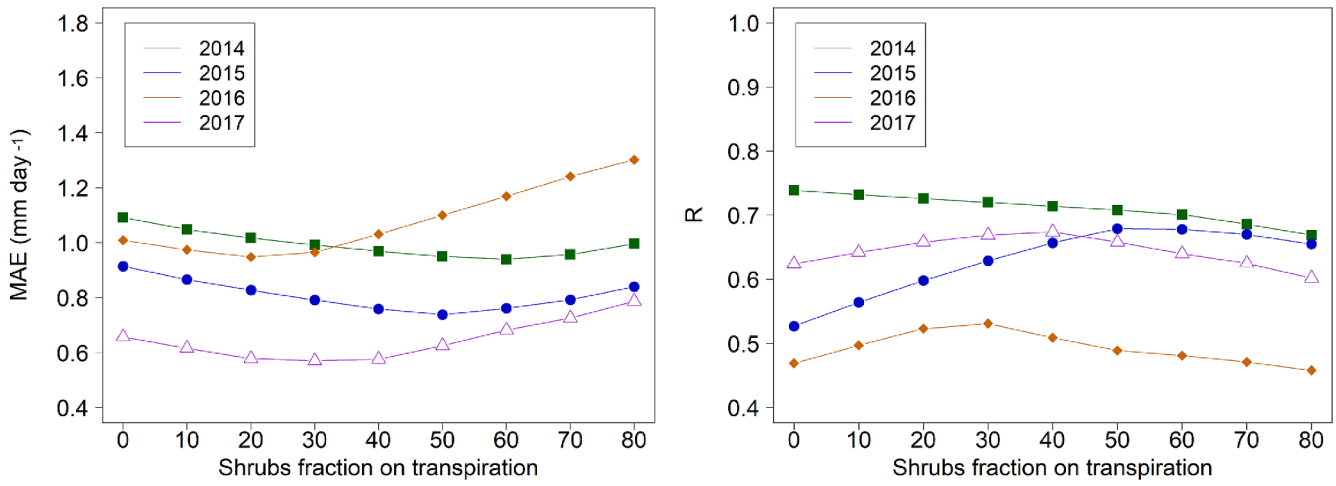

Fig. 2. Mean absolute error (MAE, left panel), and coefficient of correlation (R, right panel) versus fraction of explained total transpiration flux from simulated shrubland.

2.4.2. Model calibration

The soil hydraulic parameters reported in Table 2 ($\theta_r, \theta_s, \alpha, n, K_s$ and l, respectively residual SWC, saturated SWC, two parameters of the water retention curve, the saturated hydraulic conductivity and the tortuosity parameter) are optimized, starting from a first guess derived from ROSETTA model (Schaap et al., 2001), based on soil texture of the site, using the built-in inverse solution available in Hydrus 1D. The optimal set of parameters is reasonable, and it is sufficiently close to the set of first guess parameters. It is found through the minimization of the following objective function (Simunek et al., 1998), simplified in the present case as in Equation (1).

$$\Phi(\boldsymbol{b}, q) = \sum_{j=1}^{m_q} v_j \sum_{i=1}^{n_{qj}} w_{i,j} \left[q_j^*(\boldsymbol{x}, t_i) - q_j(\boldsymbol{x}, t_i, \boldsymbol{b}) \right]^2 \quad (1)$$

The term $\sum_{j=1}^{m_q} v_j \sum_{i=1}^{n_{qj}} w_{i,j} \left[q_j^*(\boldsymbol{x}, t_i) - q_j(\boldsymbol{x}, t_i, \boldsymbol{b}) \right]^2$ represents the deviations between measured and computed soil water content (in this paper); m_q is the number of different sets of measurements (here equal to 1, since only SWC is used); n_{qj} is the number of measurements in the measurement set; $q_j^*(\boldsymbol{x}, t_i)$ are the SWC measurements at time t_i for the measurement set at location $\mathbf{x}$; $q_j(\boldsymbol{x}, t_i, \boldsymbol{b})$ are the SWC model predictions for the vector of optimized parameters $\mathbf{b}$; v_j and $w_{i,j}$ are weights associated with a certain measurement set or point, respectively. The vector of optimized parameters contains the soil hydraulic parameters reported in Table 2. The weighting of inversion data is done by standard deviation. The weight v is defined as $1/n_j\sigma_j^2$, hence, the function Φ becomes the average weighted squared deviation normalized by the variances σ_j^2 of the measurements.

Hydrus 1D uses the Levenberg-Marquardt (Marquardt, 1963) optimization algorithm for the minimization of Φ.

For the optimization, both the vegetation configurations (either grass or shrub) were tested. Then, the shrubland configuration was selected (see Section 3.1). The calibration was performed using the measures of SWC at 20 cm and 40 cm of depth in the 2015 growing season and evaluating the goodness fit between predicted and observed SWC. That year was selected because it presented both wet and dry periods whose duration was also particularly long. Hence, the 2015 growing season contains a wide range of soil and atmospheric conditions. The model calibration was not performed on Feddes parameters to avoid more complexity and parameterization and the problem of equifinality – that is, according to Beven (1993, 2006) and Khatami et al. (2019), the ability of a model to produce comparable and satisfactory outputs with different set-ups or set of parameters.

2.4.3. Model validation

Direct simulations are performed with the single vegetation (either grass or shrubs) or the double vegetation (i.e. a mixture of the two land covers) approaches of Hydrus 1D. The direct simulations of the model are validated using the eddy covariance-derived actual evapotranspiration. Furthermore, direct simulations of the model with the double vegetation module are performed varying, year by year, the transpiration fraction explained by shrubland, which minimizes the mean absolute error and correlation coefficient between ETa measurements and simulations. This approach appears reasonable, since different growing seasons are characterized by different soil and meteorological conditions. In all simulations (grassland, shrubland, mixture of grassland and shrubland, and also in reality), no bare soil evaporation exists, because of the thick cover of grass.

2.5. Chamber measurements of ETa

The eddy covariance half-hourly ETa is compared with whole-canopy chamber transpiration (Patono et al., 2022) measurements of *Hippophae rhamnoides* performed during a field campaign on 4 September 2020 to understand how close the eddy covariance measurements are to shrubland transpiration. Chamber measurements were made using a prototype of a 'canopy-balloon' system, the Gas-Exchange System for perennial plants (b-GES), described by Patono et al. (2023). Briefly, the b-GES canopy chamber consisted in an inflated polyethylene balloon; its outlet was connected through a 2-way valve with reference-air to an InfraRed Gas Analyzer – IRGA (Li-850 with internal air sample pump, LICOR, USA) to detect water vapor fluxes in/out the chamber-air.

2.6. Statistical analyses and environmental conditions affecting simulated and observed ETa

Temporal comparisons at daily scale between modeled and observed ETa together with other variables (SWC, VPD, precipitation, net radiation, wind speed, air temperature, and soil heat flux) are performed because they can help to find differences between simulated shrubland and grassland evapotranspiration.

To understand whether the means of simulated ETa from shrubland and grassland are statistically different, and to test the differences $ETa_{Simshrub} - ETa_{Simgrass}$ and $ETa_{Simgrass+shrub} - ETa_{Obs}$ against different environmental variables, the nonparametric Wilcoxon Rank Sum Test (Kendall and Stuart, 1967) is performed. The "stats" R package (R Core Team, 2021) and "ggsignif" R package (Ahlmann-Eltze and Patil, 2021) are used to this purpose. The choice of Wilcoxon Rank Sum Test was made because the differences between the two simulated ETa, and

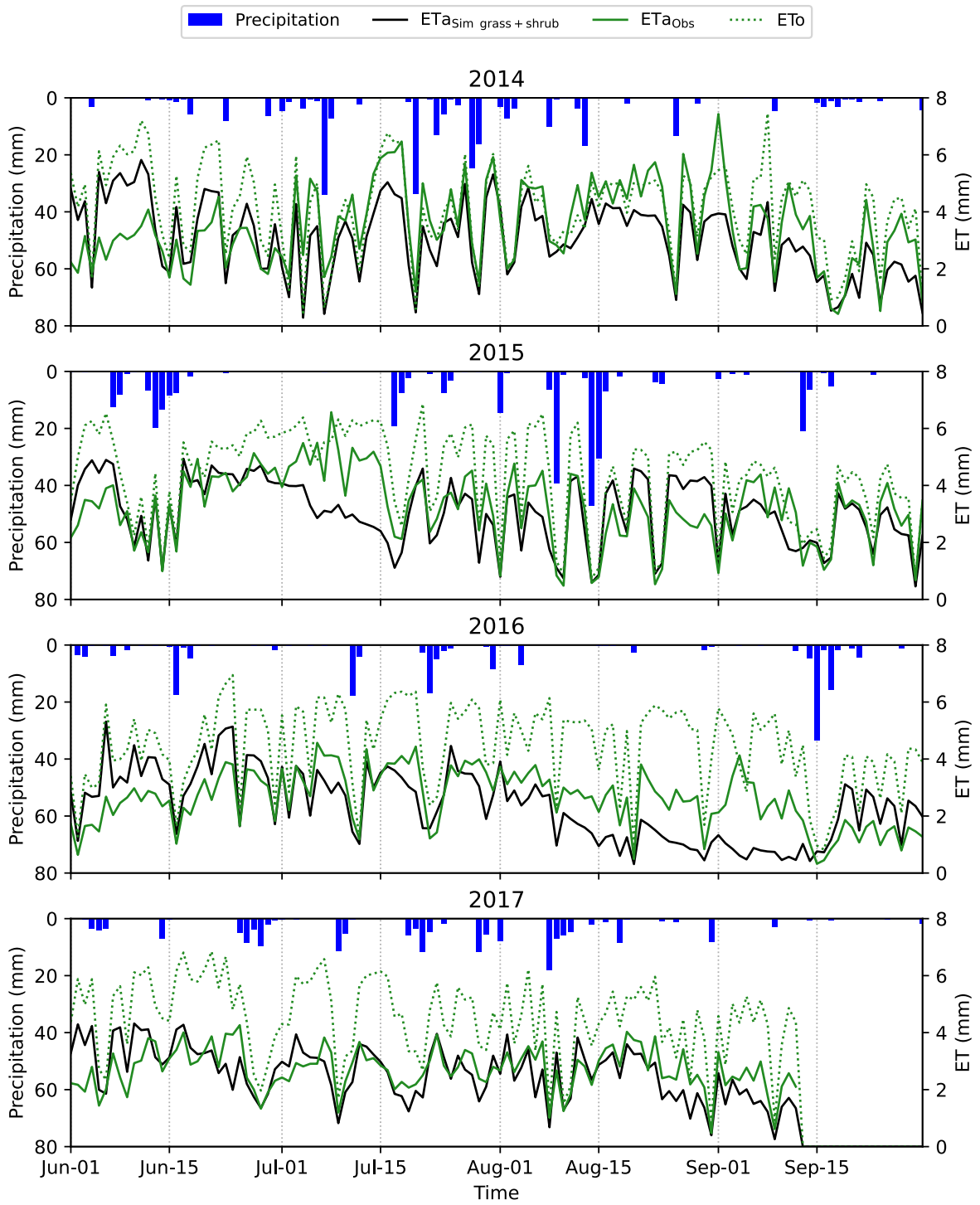

Fig. 3. Daily time series of actual evapotranspiration ETa (both modeled with Hydrus 1D double vegetation and from eddy covariance station), potential evapotranspiration (ETo), and precipitation.

between simulated and observed ETa are not normally distributed.

3. Results

3.1. Inverse modeling results

The soil hydraulic parameters are optimized using the built-in option implemented in Hydrus 1D with single vegetation. Using both the extremes of land cover (either grassland or shrubland), the best fit of measured soil water content data was obtained considering the shrubland ($R^2 = 0.69$, MWAE – Mean Weighted Absolute Error $= 0.028$ $m^3\ m^{-3}$), whereas the fit results considering grass were $R^2 = 0.49$ and MWAE $= 0.042\ m^3\ m^{-3}$. Therefore, the set of optimized soil parameters based on the shrubland optimization was used in the current study. The obtained set was within the range of expected values for the soil type at the site, and coherent with other studies (e.g. Bertoldi et al., 2014; Dai et al., 2019).

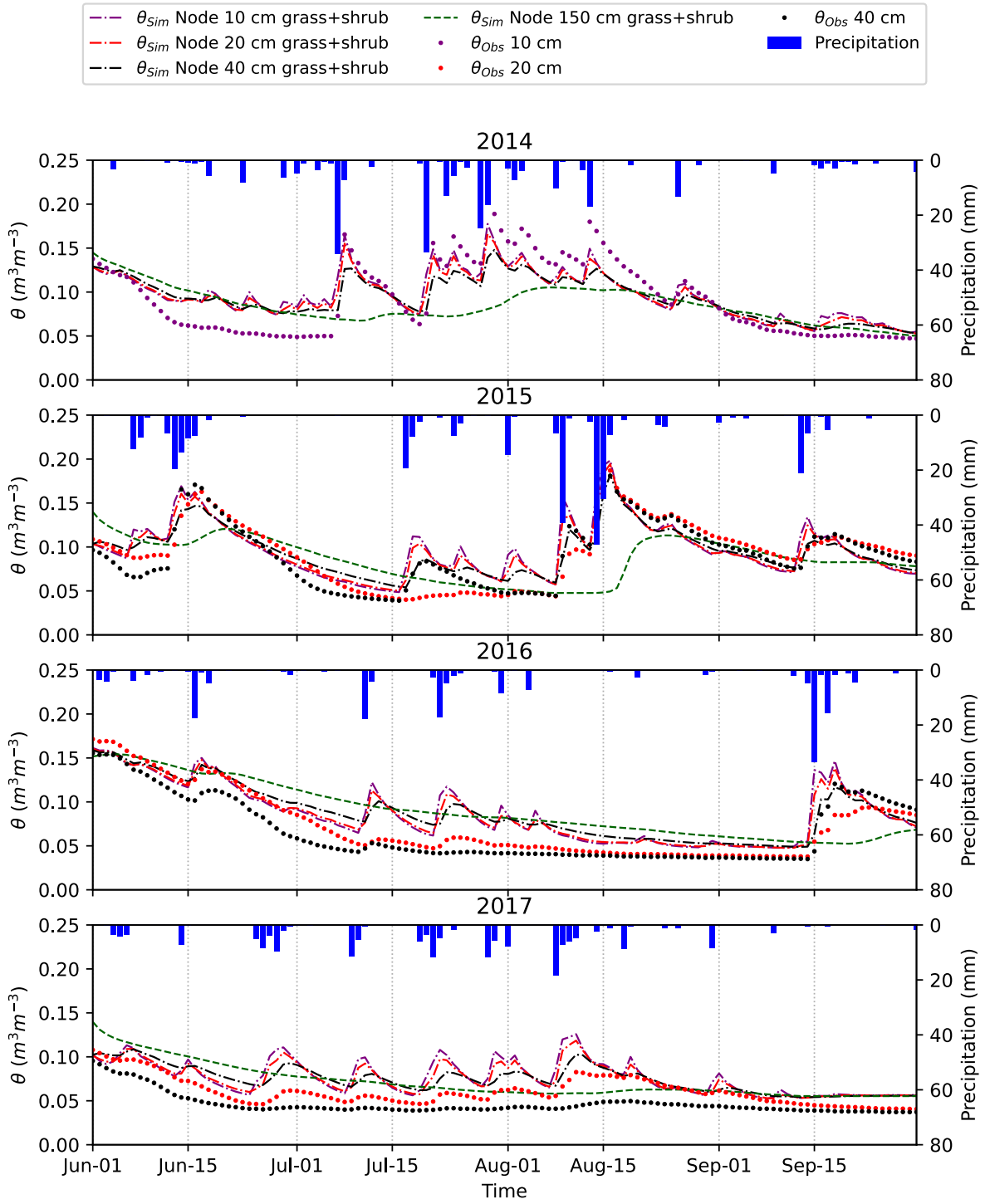

Fig. 4. Daily time series of precipitation, measured (θ_{obs}) and modeled (θ_{Sim}) SWC from the simulation with double vegetation at the observation nodes of 10, 20, 40 and 150 cm (measures at 150 cm are not available).

3.2. Validation of Hydrus 1D with double vegetation

The Hydrus 1D model with double vegetation yields good results regarding ETa. The model output is evaluated with two metrics, namely the coefficient of correlation (R) and the mean absolute error (MAE) for several fractions of transpiration flux explained by shrubland (from 0 % to 80 %, Fig. 2). It should be noted that the fraction of explained total transpiration flux from either grassland or shrubland is not the area coverage of the two vegetation types.

The fraction of the total transpiration flux assigned to shrubland could reasonably be between 20 % and 50 % (depending on the growing season characteristics), because the MAE tends to be lower in that range (with only 2014 as an exception, when the lowest MAE is found with 60 % of explained transpiration by shrubland). The negative trend of MAE found in 2014, in the range 0–60 % of transpiration flux explained by shrubland, could be due to the high-water availability (therefore, an energy-limited ETa regime), which would have caused a better agreement between the eddy covariance data and a land cover mainly characterized by shrubland.

The correlation coefficient decreases in every analyzed growing

Table 3
MAE and R coefficient for the modeled SWC (with Hydrus 1D "double vegetation") compared with measurements in the four growing seasons. N/A indicates not available values because of non-existent observations.

	Soil depth					
	10 cm	20 cm	40 cm	10 cm	20 cm	40 cm
	MAE ($m^3\ m^{-3}$)			R (−)		
2014	0.018	N/A	N/A	0.90	N/A	N/A
2015	N/A	0.017	0.013	N/A	0.82	0.92
2016	N/A	0.016	0.024	N/A	0.91	0.89
2017	N/A	0.015	0.028	N/A	0.75	0.73

season for shrubland fraction on transpiration flux greater than 50 %. Optimal values for R are found for an explained transpiration fraction between 20 % and 60 %. By means of visual inspections at the site, this result appears reasonable.

Following the results of the MAE and R analysis (Fig. 2), the double vegetation simulation is characterized by a shrubland fraction on transpiration of 60 %, 50 %, 20 % and 30 %, respectively for each one of the growing seasons from 2014 to 2017. These values were selected considering a trade-off between MAE minimization and R maximum values. The mentioned fractions appear reasonable also considering the shrubland area included within the flux footprint. In different growing seasons, the contribution of shrubland to the total transpiration flux is reasonably different, depending on the soil and meteorological conditions, and it needs modifications to fit the measured ETa. In particular, the two wet growing seasons (2014 and 2015) are characterized by lower VPD and higher precipitation and soil water content, if compared to the other growing seasons. Hence, the shrubs are likely more able to extract water, and their impact on total ETa flux is higher.

The modeled actual evapotranspiration (ETa_{Sim}) is compared to the measured ETa from eddy covariance (ETa_{Obs}). The modeled SWC is compared against the measured one. For 2015, 2016 and 2017 measurements at two depths (20 and 40 cm) are available and therefore both modeled shrubland and grassland SWC are compared with measures at those two depths. For the 2014 growing season, the model computation and comparison with measures occur at 10 cm of depth. The model is able to reproduce satisfactorily the observed ETa (also in terms of oscillations, Fig. 3) and the observed SWC (Fig. 4 and Table 3). Exceptions are particularly found in dry, long periods (as in 2015 and 2016), when the lack of precipitation reduces the fit of the model. Moreover, the model tends to be oversensitive to precipitation events if compared to measured data. This is particularly evident in 2017.

In general, the cumulative ETa agreement is good, despite the underestimation of cumulative simulated ETa (Fig. 5). In particular, the growing season cumulative error of the simulated ETa with double vegetation is, compared to ETa_{Obs}, −37.7 mm, −21.7 mm, −42.0 mm, and −13.0 mm, respectively in the four growing seasons.

3.3. Simulations with a single vegetation land cover

3.3.1. Observed and simulated evapotranspiration from different land covers

Generally, a slightly higher agreement is found between the observed evapotranspiration (ETa_{Obs}) and the simulated shrubland ($ETa_{Sim\ shrub}$), when compared to the simulated grassland ($ETa_{Sim\ grass}$), as illustrated in

Table 4
Coefficient of determination and mean absolute error between observed and modeled ETa.

R^2	MAE mm d^{-1}	Land cover	Year
0.46	1.12	Grass	**2014**
0.37	1.01	Shrub	
0.28	0.91	Grass	**2015**
0.47	0.83	Shrub	
0.22	1.01	Grass	**2016**
0.33	1.12	Shrub	
0.39	0.65	Grass	**2017**
0.34	0.78	Shrub	

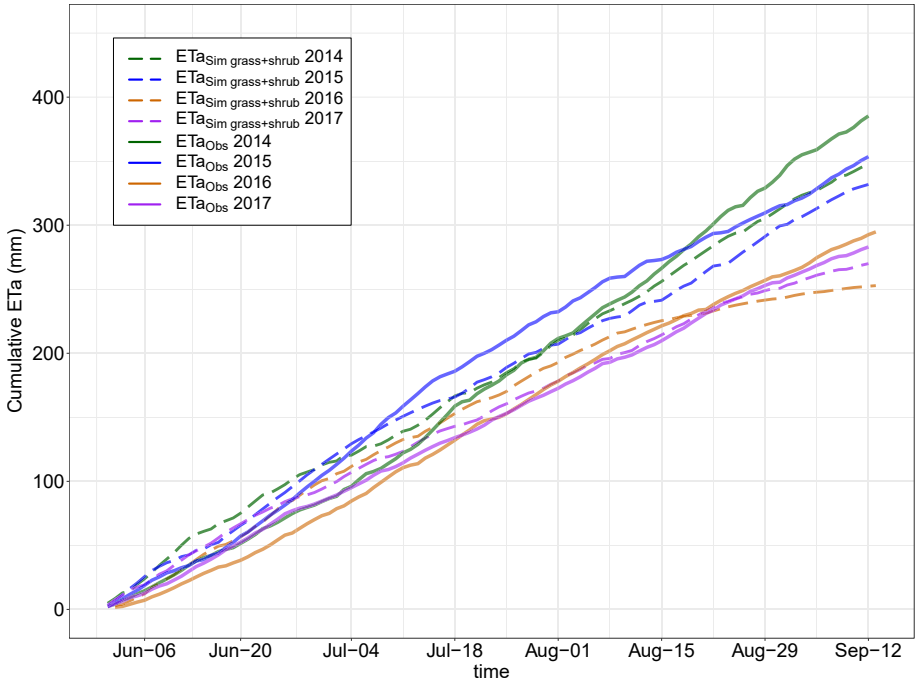

Fig. 5. Cumulative actual evapotranspiration as modeled by Hydrus 1D double vegetation ("grass + shrub", mixture of grassland and shrubland) and from eddy covariance measures.

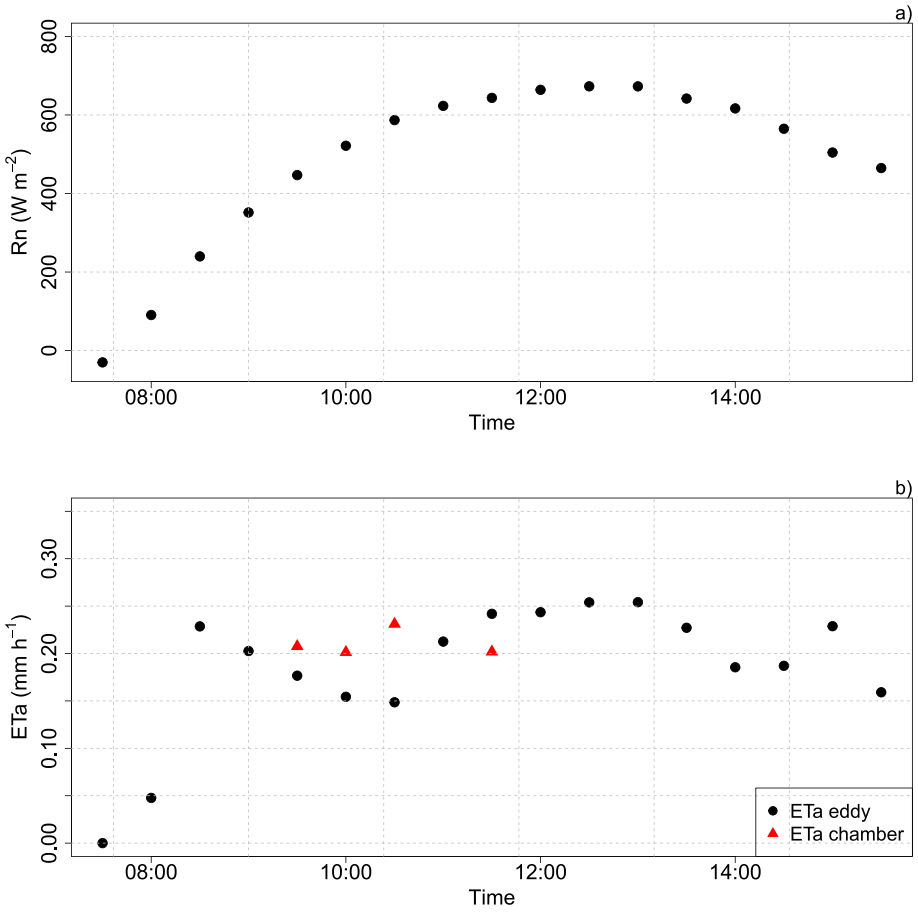

Fig. 6. Comparison between eddy covariance-derived and chamber ETa (a) and R_n data for 4 September 2020 (b).

Table 4. It should be noted that R^2 and MAE are not necessarily anti-correlated, so a decrease in R^2 may not correspond to a decrease in MAE and vice versa. Moreover, the differences between simulated shrubland ETa and simulated grassland ETa are statistically significant in each growing season.

An inter-annual variability of the simulation performance is found. Considering the MAE, in overall wetter growing seasons, the error is clearly lower in the shrubland case. This might be due to the fact that shrubs were able to extract more water from deeper soil layers. In the two dry growing seasons (2016 and 2017), the MAE of shrubland simulations is higher than the one found for grassland simulations. This behavior might be due to the model inability to correctly reproduce the drying process in the long dry period between August and September 2016. For 2017, the problem might be in the already mentioned model oversensitivity to relatively small precipitation events.

The modeled and observed ETa time series show an agreement which is again year-dependent. The relatively high R^2 in 2014 for grassland simulation can be due to the wet and cold conditions, whereas on average the simulated shrubland shows a higher R^2, compared to grassland. The lower performance of grassland simulations in 2015 and 2016 might be due to the presence of two long dry periods with almost no precipitation. In 2017, although being characterized by overall drier conditions if compared to 2014, a more well-distributed but weak precipitation occurred. So, the two simulations have a comparable R^2.

The agreement between shrub transpiration and eddy covariance measurements is also found in a specific field campaign performed on 4 September 2020. This campaign was characterized by a sunny day with high available radiation (Fig. 6a). Although short, the campaign illustrates that at the Cogne site, the eddy covariance measurements are close to the measurements of transpiration from four *Hippophae rhamnoides* plants (Fig. 6b). The difference between chamber and eddy covariance ETa mean values is 0.03 mm h^{-1}. On average, the eddy covariance measurements indicate a lower ETa if compared to chamber measurements because of the smoothing effect of the flux footprint, which includes a mixture of shrubland and grassland.

The tendency suggested by the model outcomes for a simulated shrubland, that is, the shrubland is affecting ETa, appears confirmed.

The two modeled land covers show different behaviors and, in general, a higher ETa is found considering the shrubland, as also illustrated by the daily (Fig. 7) and cumulative (Fig. 8) values over the growing seasons. With reference to Fig. 7, long dry spells (as the one in 2015) highlight the strong ETa decrease from simulated grassland, whereas the simulated ETa from shrubland remains high as the observations. However, with even longer dry conditions as in the period August-September 2016, preceded by low precipitation, the model performance decreases dramatically also for the simulated grassland. Higher daily ETa from shrubland is found if compared to grassland.

With reference to Fig. 8, the cumulative ETa shows important differences of 79.1, 73.4, 61.7, and 57.0 mm between simulated ETa from the shrubland and from the grassland, highlighting a higher ETa from the shrubland.

Fig. 9 shows the sensitivity of measured and modeled ETa to SWC. In the lower range (water-limited), the sensitivity of the simulated grassland ETa is generally higher than those of the simulated shrubland and of the observed one. The energy limitations for higher SWC are also clear.

3.4. Environmental conditions affecting observations and simulations

Using EF and simulated soil water content within the 0–100 cm

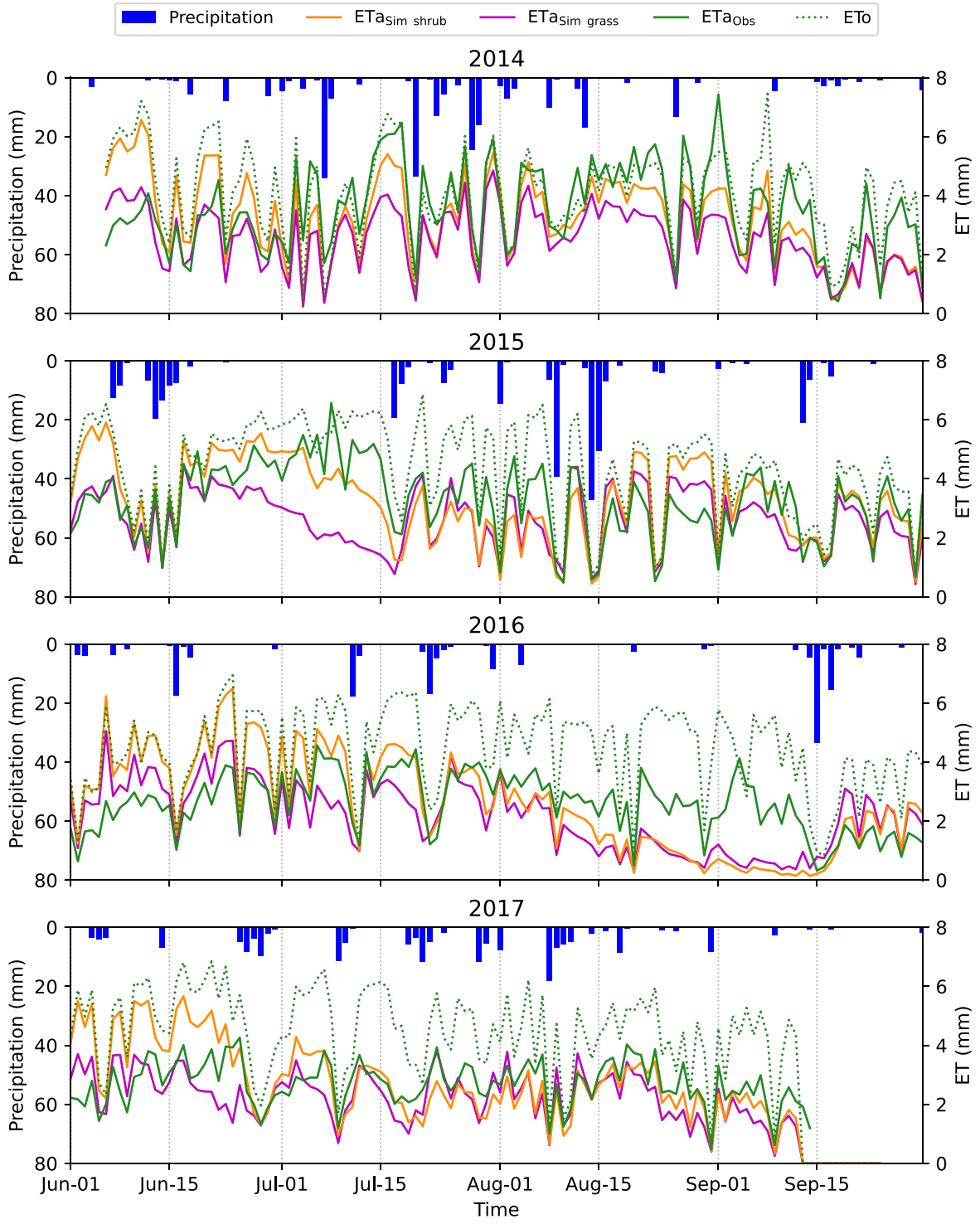

Fig. 7. Daily time series of actual evapotranspiration from eddy covariance (ETa$_{Obs}$), modeled actual evapotranspiration from single vegetation simulations (ETa$_{Sim\ grass}$, ETa$_{Sim\ shrub}$), potential evapotranspiration (ETo) and precipitation for the four analyzed growing seasons.

profile, a confirmation of the energy-limited regime of ETa was found at the site, despite the low precipitation inputs, except in 2016, when an evident water-limited regime was noticed below 0.07 $m^3\ m^{-3}$ (Fig. 10).

Looking at temporal series of ETa deviations and of VPD (which depends on air temperature and relative humidity), enhanced differences between model outputs and observations are found when VPD peaks occur, and when the soil is generally dry. The phenomenon is particularly evident when long dry periods occur (Fig. 11). The considered deviations are between the observed and double vegetation simulated ETa, and also between simulated ETa from either grassland or shrubland.

A shift towards higher deviations $ETa_{Obs} - ETa_{Simgrass+shrub}$ is confirmed at high VPD values (although frequently the differences among VPD classes are not significant or significant at a low level, as illustrated in Fig. 12, panels a), d), g), h)). The net radiation did not yield any particularly significant difference among groups, with only one notable exception (Fig. 12, Panels b), e), h), k)). In addition, at high R_n values, generally the dispersion of deviation values increases in the

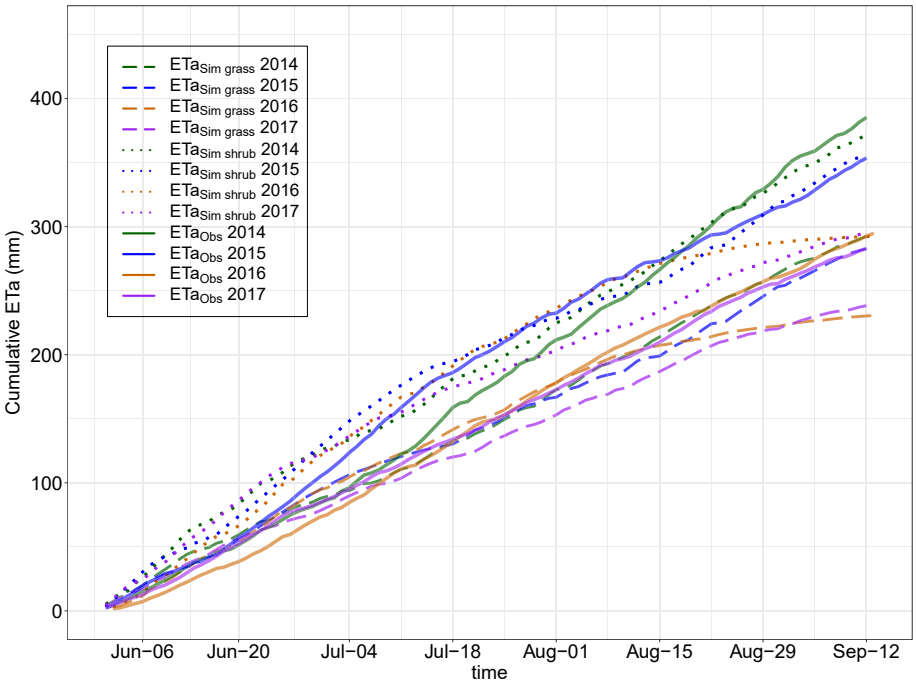

Fig. 8. Cumulative values of observed and simulated actual evapotranspiration from either simulated shrubland or grassland.

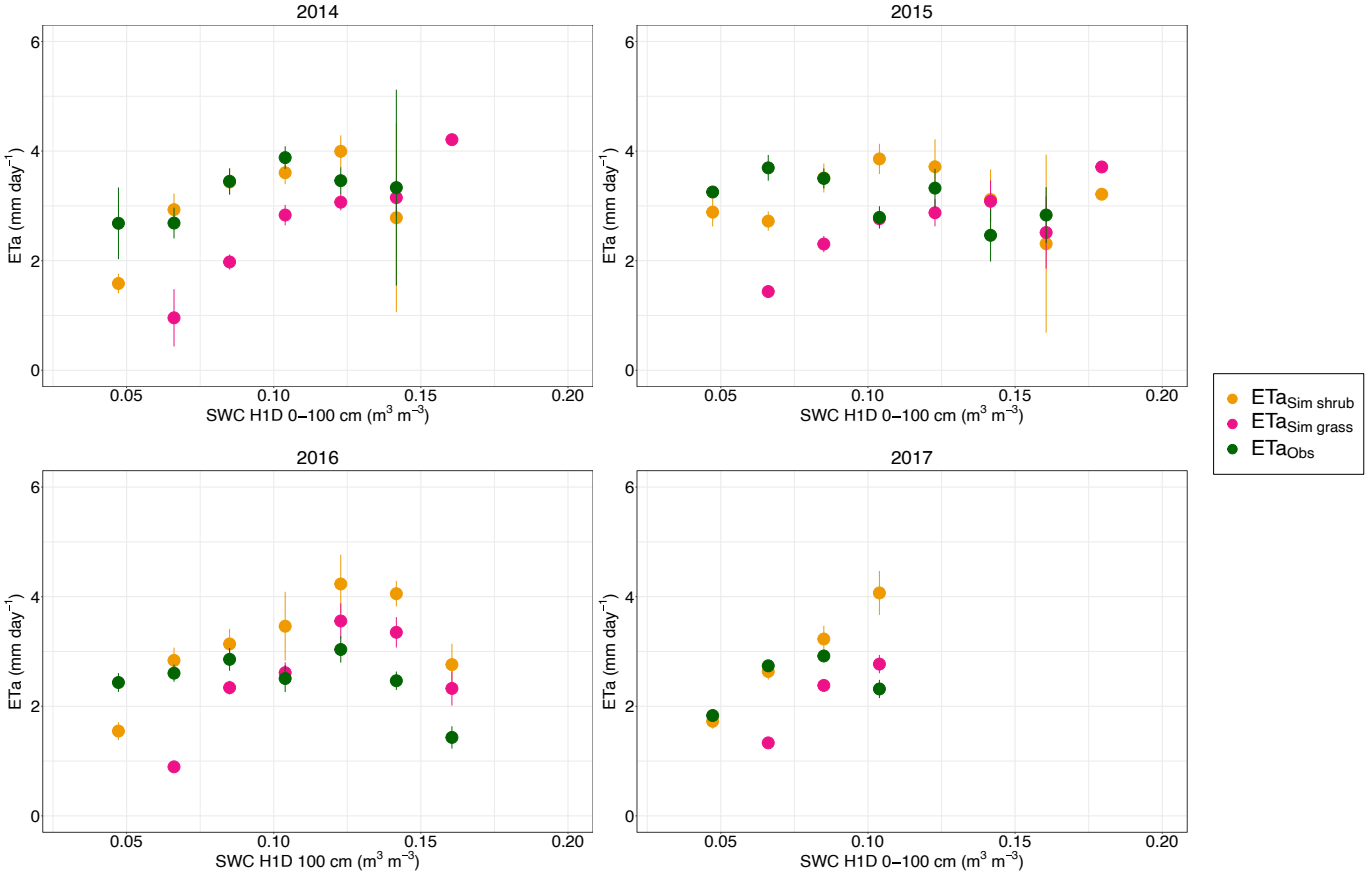

Fig. 9. Binned scatterplot of eta of simulated shrubland and grassland, and observed eta, compared with soil water content within the 0–100 cm horizon. In the case of simulated shrubland and grassland, the soil water content of the respective simulations is reported. In the case of observed ETa, the 0–100 profile is obtained from the double vegetation simulation (mixture of grassland and shrubland). The error bars represent, for each point, the mean standard error.

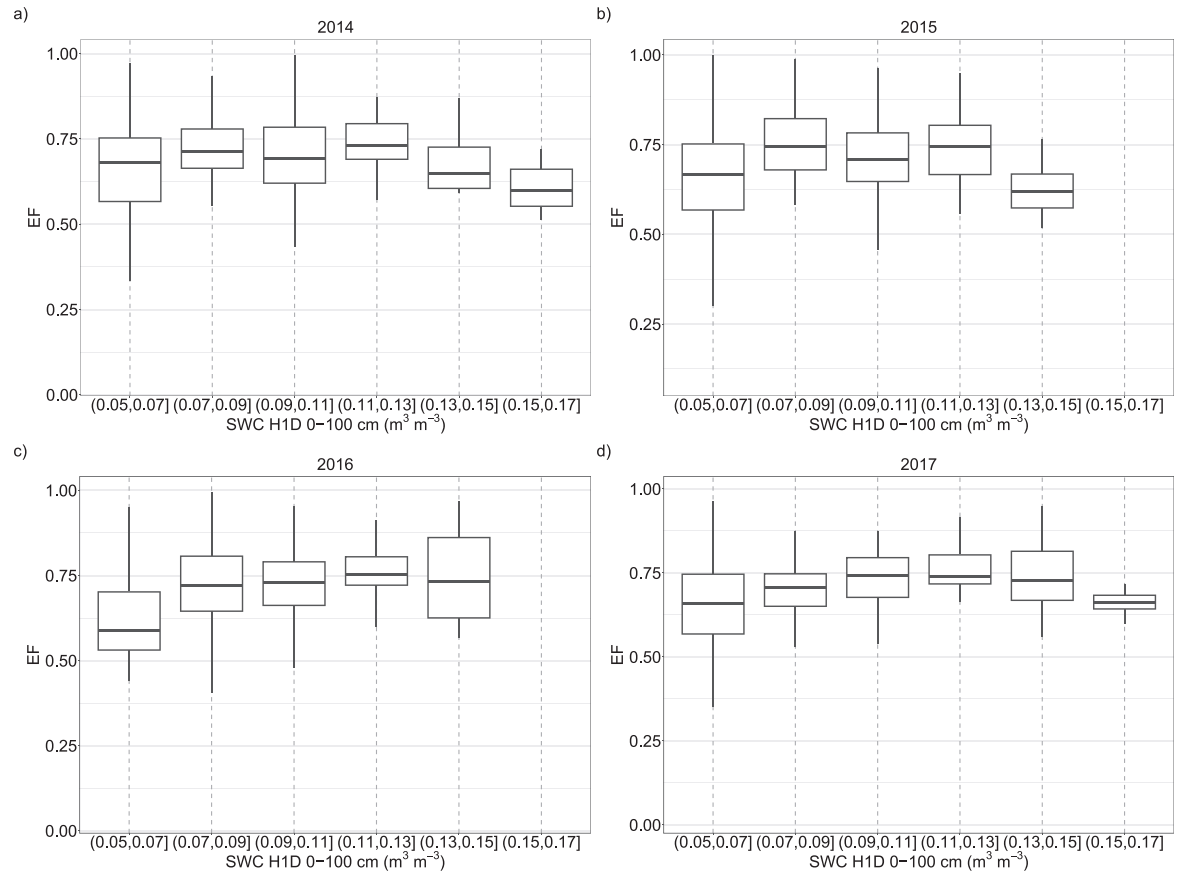

Fig. 10. Boxplots of evaporative fraction (between 10:00 and 15:00 local time, UTC + 1) versus simulated soil water content within the 0–100 cm horizon.

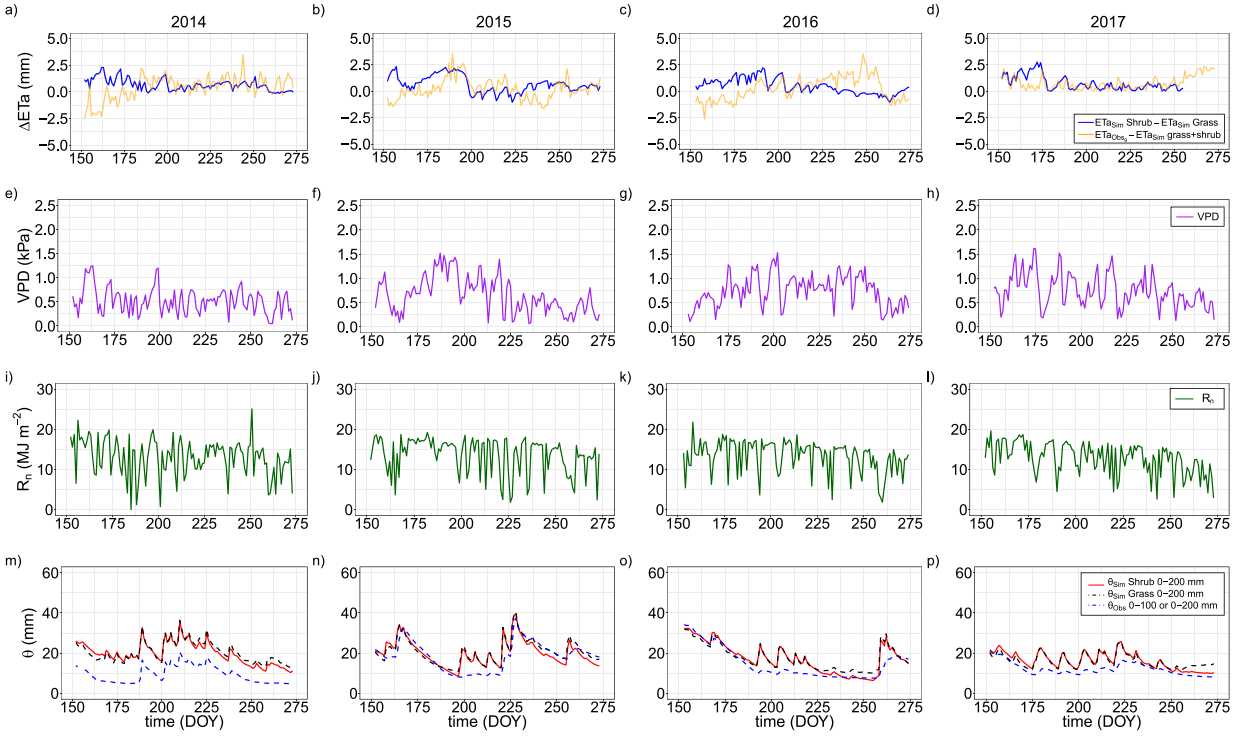

Fig. 11. Deviation between the modeled actual evapotranspiration ($ETa_{Simgrass}$ or $ETa_{Simshrub}$) and between modeled and eddy covariance (ETa_{Obs}) evapotranspiration (a–d). VPD values (e–h), net radiation (i–l) and modeled and observed 20 cm SWC from shrub and grass, respectively $\theta_{Simshrub}$ and $\theta_{Simgrass}$ (m, n, o p). To make the figure more readable, the dates are expressed as Julian days (DOY, day of year).

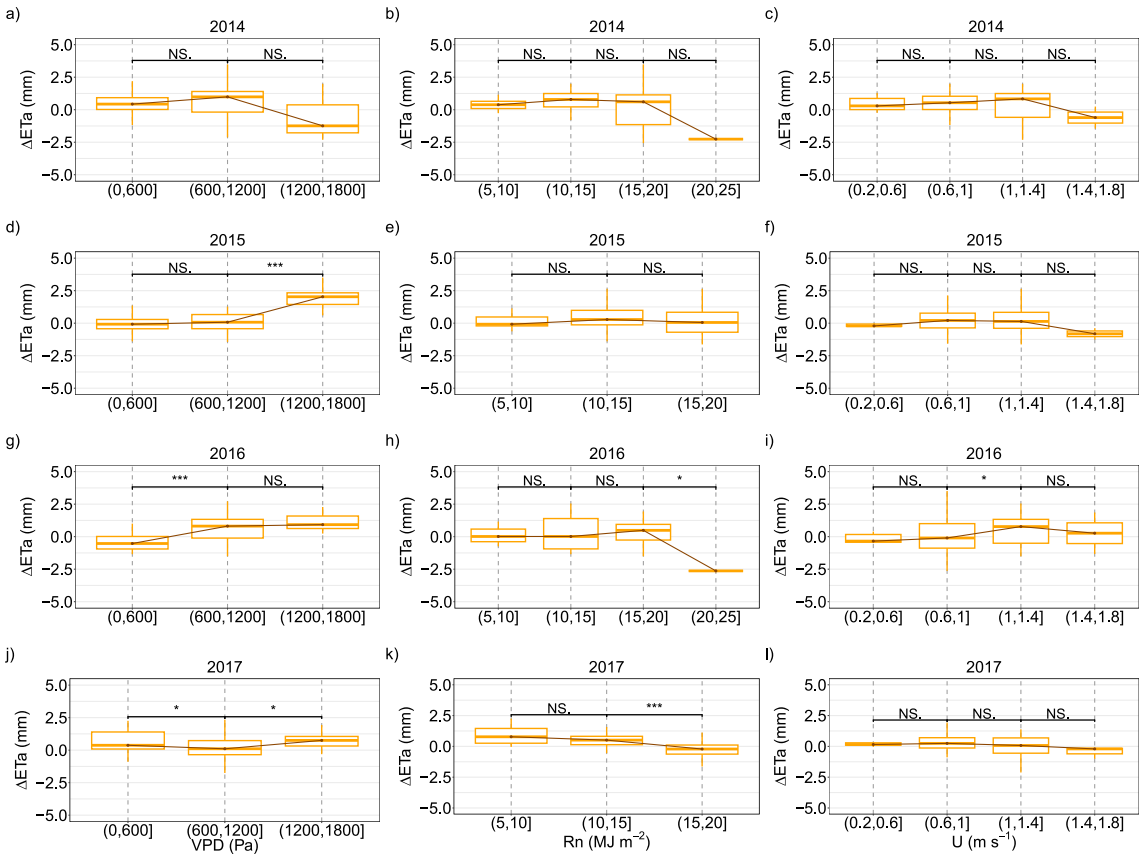

Fig. 12. Boxplots of the ETa deviations between measured and modeled ETa with the double vegetation approach of Hydrus 1D as a function of several micrometeorological variables (panels a, d, g, j: vapor pressure deficit – VPD; panels b, e, h, k: net radiation – R_n; panels c, f, i, l: wind speed – U) in the four considered growing seasons. Dark orange line indicates the boxplots median trend. The significance of boxplot differences as a function of classes of the micrometeorological variables is also indicated (NS: not significant; *: significant with p-value between 0.01 and 0.05, ** significant with p-value between 0.001 and 0.01, *** highly significant, with p-value lower than 0.001). (For interpretation of the references to colour in this figure legend, the reader is referred to the web version of this article.)

wetter growing seasons, when more frequent cloudy days occur.

Differences of ETa versus wind speed classes did not have any significance except for the low significance found in 2016 (Fig. 12, panels c), f), i), l)). The trend of $\Delta ETa_{Obs-Sim}$ with U classes varied from nearly stationary (2014, 2016) to negative (2015, 2017).

Positive patterns of the difference between observations and the simulated ETa with double vegetation approach, compared against air temperature classes, are found in 2015 and 2016 (Fig. 13, panels a), c), e), g)). Those two growing seasons were characterized by long dry periods. Less clear patterns exist considering G_0 (Fig. 13, panels b), d), f), h)), with the notable exception of 2016. In addition, the magnitude of deviations can be higher (in absolute value) with high air temperature and surface ground heat flux, but the pattern does not appear always clearly.

The deviations between the two simulated ETa (from either grassland or shrubland) show statistically significant differences for increasing VPD classes with only one exception in 2016 (Fig. 14, Panels a), d), g), j)). Highly significant deviations are found for net radiation in all growing seasons except 2017. However, in 2014 and 2016 not all the deviations are significant (Fig. 14, Panels b), e), h), k)).

Regarding wind speed, the number of non-significant deviations increases in dry and warm growing seasons. Highly significant and significant deviations are found in 2014, 2015 and in 2017 (Fig. 14, Panels c), f), i), l)). A very low significance of deviations was found especially for G_0 and T_{air} (Fig. 15). Only two notable exceptions are found in 2014 for T_{air} and in 2015 and 2017 for G_0.

4. Discussion

4.1. Modeled and observed daily soil water content and evapotranspiration

The simulated SWC shows an acceptable agreement with measures, with outcomes comparable with the findings obtained by Bertoldi et al. (2014) using GEOtop model and by Wegehenkel and Beyrich (2014) using Hydrus 1D model. The aforementioned models were both run for grasslands, but for simpler cases.

Considering ETa, the current study is comparable with the high-Andean study of Ochoa-Sánchez et al. (2019). In that paper, the case of the HBV-light model shows a higher coefficient of determination ($R^2 = 0.77$), but other models yield lower R^2 (range between 0.06 and 0.52). Bottazzi et al. (2021) found a high agreement with eddy covariance measurements using the GEOframe-Prospero model ($R^2 > 0.85$). Nevertheless, GEOframe is a large-scale model, whereas in the current study a less time-consuming approach is used to explain the ecosystem behavior. The Hydrus 1D approach is sufficient, although improvements could be done especially with field campaigns focused on the soil properties (i.e. direct measures of θ_s). The relationships between eddy covariance-derived ETa and simulations yielded a lower agreement if compared to Wegehenkel and Beyrich (2014), where the ETa was simulated with Hydrus 1D model but on a simpler case: a managed grassland. The comparison of simulated and eddy covariance ETa yielded higher R^2 values ranging from 0.60 to 0.74, depending on the model configuration. It should be pointed out that the site was characterized by only one land cover and it was located on a homogeneous and flat

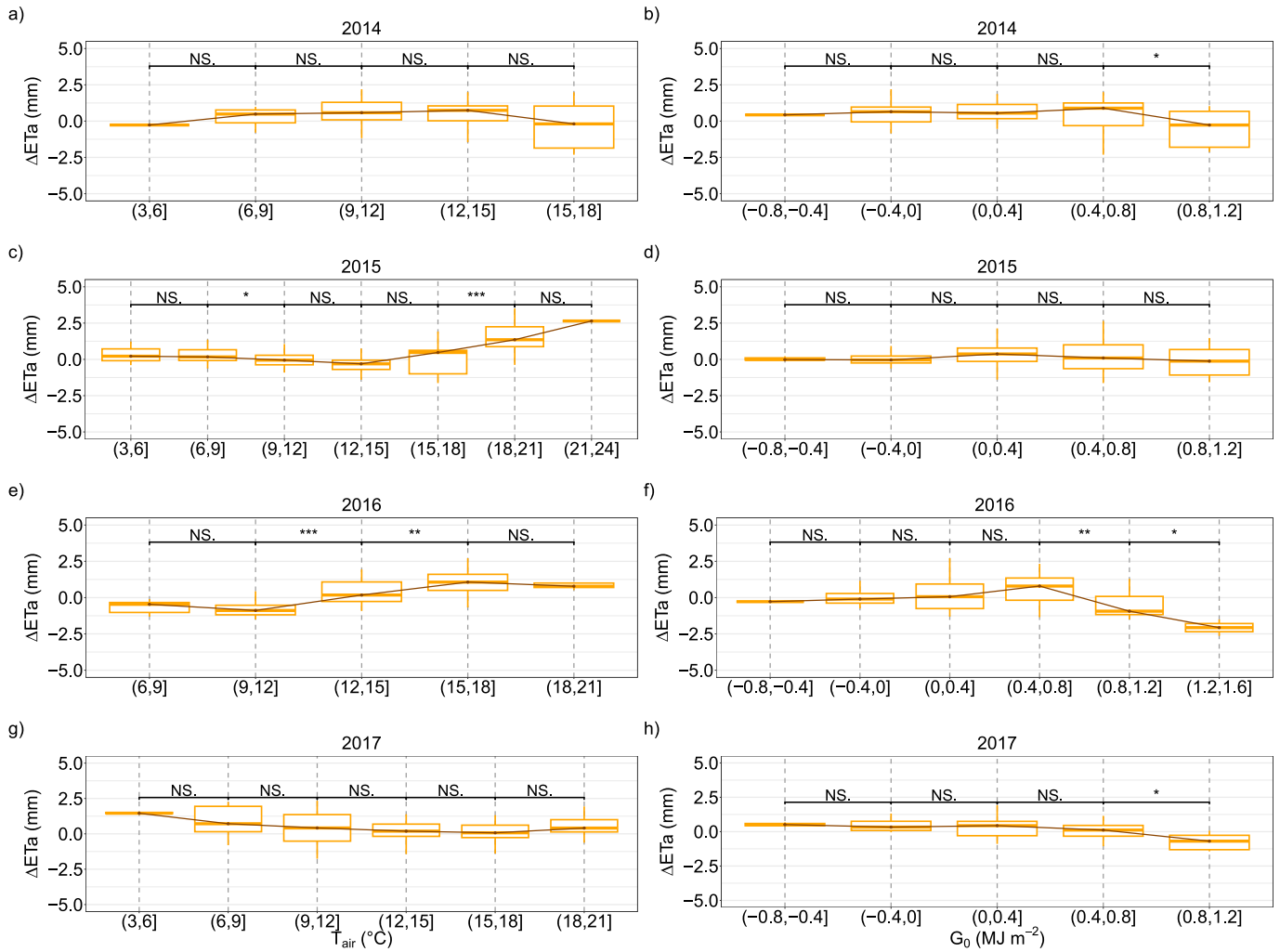

Fig. 13. Boxplots of the deviations between eddy covariance and simulated (with double vegetation approach) ETa as a function of air temperature (T_{air}, panels a, c, e, g) and ground heat flux at the surface (G_0, panels b, d, f, h) in the four considered growing seasons. Dark orange line indicates the boxplots median trend. The significance of boxplot differences as a function of classes of the micrometeorological variables is also indicated (NS: not significant; *: significant with p-value between 0.01 and 0.05, ** significant with p-value between 0.001 and 0.01, *** highly significant, with p-value lower than 0.001). (For interpretation of the references to colour in this figure legend, the reader is referred to the web version of this article.)

terrain.

As illustrated in Section 3.3.1, the daily time series of $ETa_{Sim\ shrub}$ show a better agreement with ETa_{Obs}, if compared to $ETa_{Sim\ grass}$. The lowest agreement is in 2016, and this might be related to the long dry periods of that growing season. A higher R^2 of $ETa_{Sim\ grass}$ compared to ETa_{Obs} in 2014 is also found, however that year was a wet growing season, hence the grass activity was enhanced.

All simulations (grassland, shrubland, double vegetation) provided lower than measured ETa values, during 2015 and especially the dry 2016 periods. This could suggest the optimization of the Feddes parameters for root water uptake. However, the simultaneous optimization of both soil hydraulic and Feddes parameters was out of the scope of the paper, being the main goal to investigate, with fixed soil and vegetation parameters, the sensitivity of the model to the two types of vegetation and to test the double vegetation model, without adding more complexity and (over)parameterization to the study.

The cumulative values of observed ETa during the considered growing seasons are comparable with the annual values reported for the Torgnon ICOS – LTER site (having the range 400–700 mm) by Bottazzi et al. (2021).

4.2. Impact of shrubland on actual evapotranspiration

The results of the current study suggest that the observed mixture of grassland and shrubland at the Cogne site significantly affects evapotranspiration. Moreover, the shrubland would likely cause an actual evapotranspiration increase of up to a maximum of 79 mm in 2014 compared to the grassland. An increase in ETa was also found by van den Bergh et al. (2018). The measured ETa in the current study (mean value 3 mm day^{-1}, range 0.30–7.4 mm day^{-1}) are close to the values ranging from almost 3 mm day^{-1} to almost 8 mm day^{-1} found by van den Bergh et al. (2018) for *Alnus* shrubland and grassland. However, the range observed at Cogne is wider. The ETa_{Obs} average values found at Cogne are higher than the values (range 1.9 – 2.2 mm d^{-1}) reported by Gu et al. (2008).

In the current study, the modeled ETa from shrubland is on average 3.2 mm day^{-1} (range 0.14–6.6 mm day^{-1}) and the modeled ETa from grassland is on average lower with 2.5 mm day^{-1} (range 0.24–5 mm day^{-1}). At Cogne, the average difference between grassland and shrubland simulated daily ETa is 0.65 mm day^{-1}, which is lower than the value of 1.2 mm day^{-1} reported by van den Bergh et al. (2018).

In three of four growing seasons, the ETa_{Obs}/P ratio of each hydrological year was around 45 % (47 % in 2015, 46 % in 2016, 45 % in

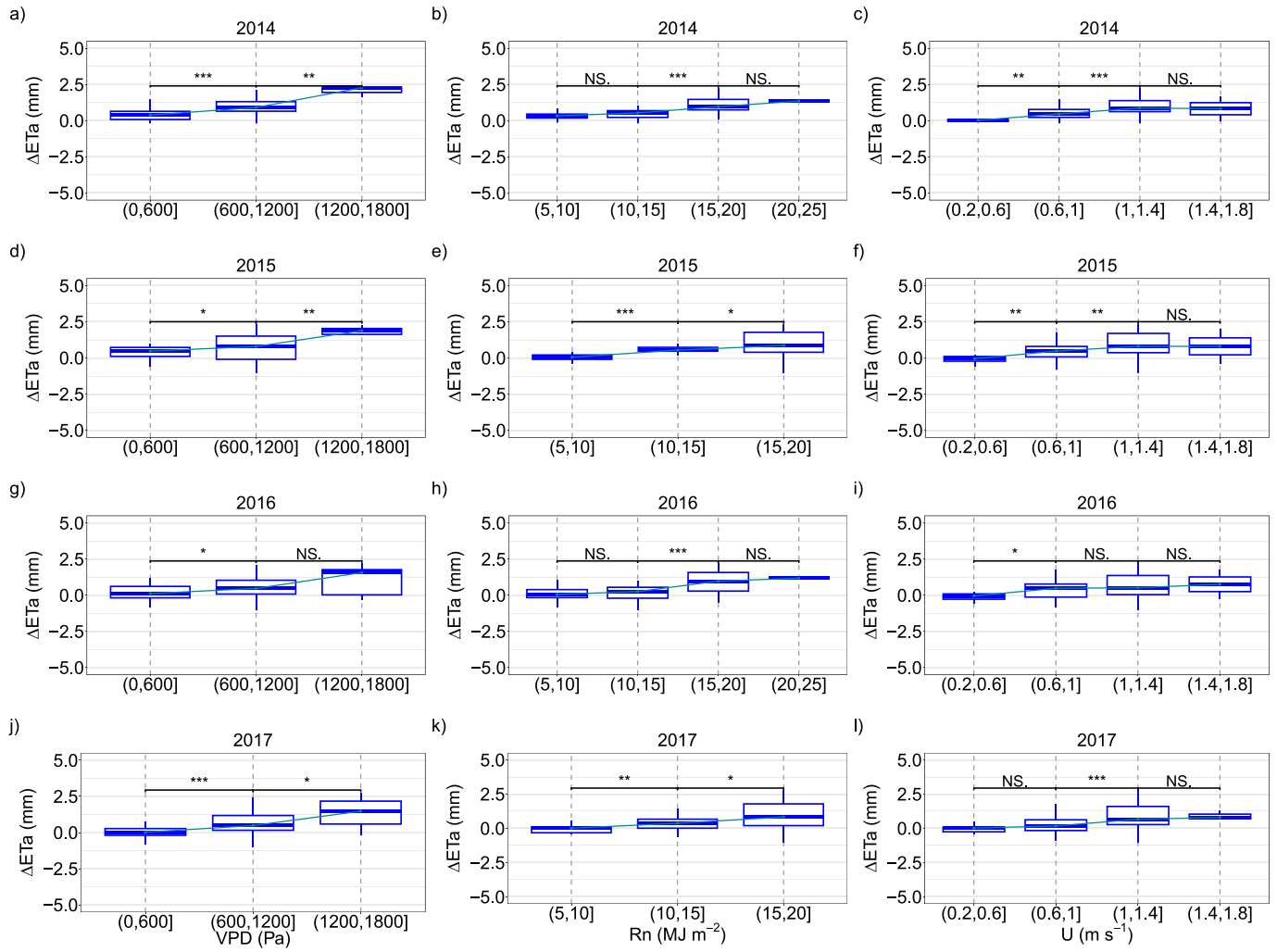

Fig. 14. Boxplots of the deviations $ETa_{Simshrub} - ETa_{Simgrass}$ as a function of several micrometeorological variables (panels a, d, g, j: vapor pressure deficit – VPD; panels b, e, h, k: net radiation – R_n; panels c, f, i, l: wind speed – U) in the four considered growing seasons. Light blue line indicates the boxplots median trend. The significance of boxplot differences as a function of classes of the micrometeorological variables is also indicated (NS: not significant; *: significant with p-value between 0.01 and 0.05, ** significant with p-value between 0.001 and 0.01, *** highly significant, with p-value lower than 0.001). (For interpretation of the references to colour in this figure legend, the reader is referred to the web version of this article.)

2017) which is comparable with Caviezel et al. (2014). Except for 2014, where the ratio reached 55.4 %. On the other hand, the ETa_{Obs}/P ratio reached lower maximum values than the findings of Gu et al. (2008), where a ratio close to 60 % is reported, and of Wieser et al. (2008), with reported ETa_{Obs}/P ratios within the range 51–91 %. It should be pointed out that, in the mentioned studies, the ratio is referred to the annual evapotranspiration and not to the growing season only.

For the simulations, the ratio $ETa_{Simgrass}/P$ ranges from 36 % to 42 %, whereas the $ETa_{Simshrub}/P$ ratio is always greater, ranging from 45.7.% to 53.3 %. These simulations show an evident increase of the ETa_{Sim}/P ratio in the case of shrubland, if compared to grassland (the percentage increase is +27.1 %, +25.8 %, +26.7 % and 24.1 %, respectively for the four growing seasons). This finding is very different from what was reported by Caviezel et al. (2014). In that study, slight differences were found between shrubland and grassland, with the annual ETa_{shrub}/P being almost equal to annual ETa_{grass}/P (41.1–42.6 %, respectively). The results show that the ETa depends on the site and the type of shrubland vegetation. In addition, the double vegetation simulations show a transpiration fraction explained by shrubs to total ETa higher (range: 30–60 %) than recent studies (24 % according to Wang et al., 2018). Besides, in the current study a strong inter-annual variation is found. The use of models at large scale should consider different species of shrubs and should especially keep in mind the difference between isohydric or anisohydric shrubs and their different response, that is, on one hand isohydric strategy implies a constant midday leaf water potential throughout stomata regulation. On the other hand, anisohydric strategy implies a higher duration of stomata opening with high photosynthetic rates (Sade et al., 2012). With the second strategy, the soil water depletion could be higher, and the vegetation might experience severe stress and have a higher mortality, if compared to isohydric vegetation.

4.3. Environmental conditions affecting simulations and observations

The simulations show an ETa underestimation in long dry periods and the cumulative ETa of the growing seasons, although reliable, is characterized by an underestimation at the end of the season in 2014, 2016 and 2017 (hence, when dry periods occur in the late growing season). Instead, in 2015 there is not underestimation at the end of the growing season because of high precipitation events occurred in the first half of August.

The impact of VPD and net radiation (R_n) on both observed and simulated ETa depends on the fact that the Cogne site is mostly energy-limited, as commonly found in mountainous areas (e.g. Carrer et al., 2019; Della Chiesa et al., 2014). The current study also improves the

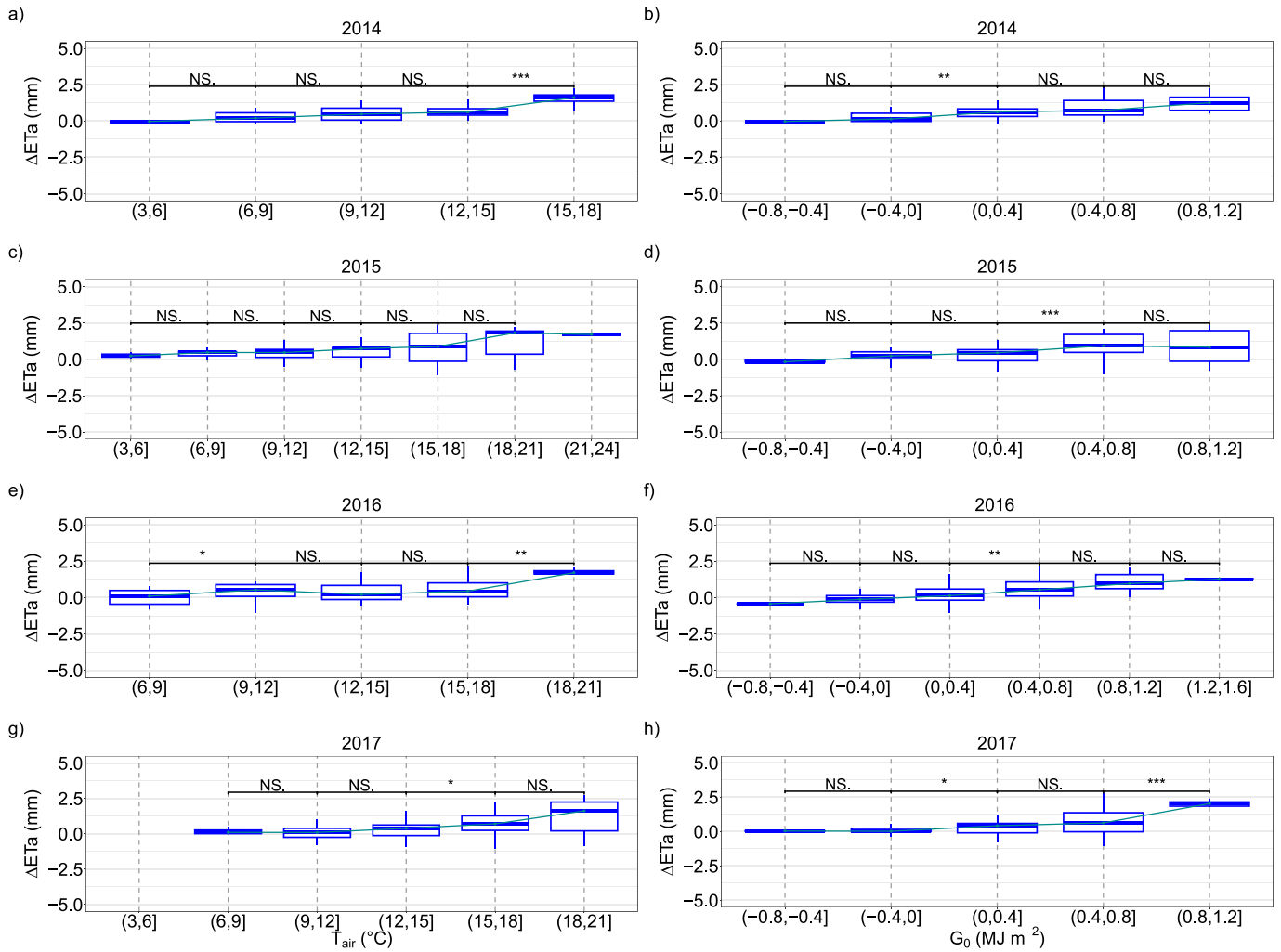

Fig. 15. Boxplots of the deviations $ETa_{Simshrub} - ETa_{Simgrass}$ as a function of air temperature (T_{air}, panels a, c, e, g) and ground heat flux at the surface (G_0, panels b, d, f, h) in the four considered growing seasons. Light blue line indicates the boxplots median trend. The significance of boxplot differences as a function of classes of the micrometeorological variables is also indicated (NS: not significant; *: significant with p-value between 0.01 and 0.05, ** significant with p-value between 0.001 and 0.01, *** highly significant, with p-value lower than 0.001). (For interpretation of the references to colour in this figure legend, the reader is referred to the web version of this article.)

characterization of ETa regimes using the simulated soil water content of the first 100 cm of soil, since Gisolo et al. (2022) showed that the identification of either energy or water-limited regimes with evaporative fraction (EF) is not easy, when only shallow soil water content measurements are available (until 40 cm depth). The water-limited regime found in 2016 (Section 3.4), reinforces the hypothesis of the role of shrubs deeper roots.

The energy-limited ETa regime implies that VPD and R_n are the most important ETa drivers, as also illustrated in several studies (Detsch et al., 2017; Gisolo et al., 2022; Wieser et al., 2008). Moreover, they are important variables in the Penman-Monteith formula for computing the potential evapotranspiration (ETo).

The differences between double vegetation simulations and observed ETa depends mainly on VPD, because it plays a key role in both simulations (via Penman-Monteith formula, hence affecting the upper boundary conditions of the model) and measurements. The fact that R_n does not have a high impact on the mentioned differences should be further investigated, but it should be noted that VPD explains a high fraction of measured ETa variance, if compared to R_n. Besides, if R_n is not playing a key role in ETa deviations between modeled and observed values, it is an important driver of ETa as an absolute value (Gisolo et al., 2022; Li et al., 2021a,b; Wieser et al., 2008).

Patterns towards more positive differences between shrubland and grassland modeled ETa, compared against micrometeorological variables, have been found. This result suggests that the already naturally higher ETa from shrubland compared to grassland would be higher in conditions of high VPD (always found) and high R_n (always found with a slight exception in 2017). A less clear behavior is found for the other analyzed variables (U, T_{air}, G_0), likely because, while they affect measured ETa (especially air temperature and surface ground heat flux), they have a relatively low impact in the ETo computation. The ETo is then reduced considering several factors, such as the soil water availability (soil water content, soil matric potential) and the vegetation root water uptake. This last variable depends on the vegetation properties (root depth, potential water uptake distribution function, ability to extract water given by the root-water uptake stress response function, which depends on the parameters of, in our case, the Feddes model – Feddes et al., 1978).

The modeled ETa certainly depends on the mentioned micrometeorological variables, but this dependency could be weakened by the nonlinearity of the root water uptake model. In addition, the wind direction exerts an important influence on ETa, since depending on the air mass provenance, a temperature and air humidity change can occur, thus altering both the ETo (hence, modeled ETa) and the eddy

covariance-derived ETa.

Of course, also SWC and precipitation play a major role. However, it is not possible to quantify the correlation because cause and effects do not occur at the same time, but with delayed and complex dynamics.

5. Conclusion

The current study, focused on actual evapotranspiration (ETa) modeling and eddy covariance measures, is performed on an abandoned mountain grassland encroached by shrubs, in four growing seasons. The study confirms that a combination of simulated evapotranspiration from shrubland and grassland using a Hydrus 1D model with double vegetation approach is able to simulate the daily ETa and the cumulative ETa during the growing seasons. The simulations were satisfactory even if the vegetation parameters were taken from literature and the soil parameters were optimized starting from predictions based on soil texture.

This study also illustrates that a soil hydrological model approach is able to represent and quantify the evapotranspiration increase by shrub encroachment, and the modeled ETa of a shrubland is higher (range +23.9 % – +27.1 %, depending on the growing season) than the ETa modeled for a grassland. This result suggests a possible future alteration of the hydrological cycle, with enhanced ETa. Moreover, the impact of the shrubs is already evident, since ETa chamber measurements of shrubs are close to the eddy covariance ETa.

The study concludes also that observed ETa regimes can be identified with simulated soil water content in the 0–100 horizon.

Micrometeorological conditions are expected to influence the amount of evapotranspiration. This influence was evaluated with the deviations between observed and simulated ETa with double vegetation approach or only shrubland or only simulated grassland ETa, both grouped by classes of micrometeorological variables. ETa deviations between observed and modeled values show more frequently significant changes with increasing VPD. A similar conclusion can be drawn for net radiation but only considering the deviations between modeled (from shrubland and from grassland) ETa grouped by net radiation.

Other variables (wind speed, ground heat flux and air temperature) do not show a strong and frequent impact on the difference between observed and modeled ETa, or the difference between simulated shrubland and simulated grassland. Differently from some past literature findings, the model outputs suggest that the evaporative index *(ETa/P)* is more severely affected by the presence of shrubs (the range is between +24 % and + 27 %, if compared to grassland). Further studies may deepen the knowledge on the deep soil water content and on the root water uptake parameters to improve the boundary conditions at the soil bottom and the vegetation modeling, respectively. Future hydrological modeling developments should deal with isohydric and anisohydric vegetation behavior.

CRediT authorship contribution statement

Davide Gisolo: Conceptualization, Data curation, Formal analysis, Investigation, Methodology, Software, Visualization, Writing – original draft, Writing – review & editing. **Ivan Bevilacqua:** Formal analysis, Methodology, Software, Visualization. **Alessio Gentile:** Conceptualization, Methodology, Writing – review & editing. **Justus van Ramshorst:** Conceptualization, Methodology, Writing – review & editing. **Davide L. Patono:** Data curation, Investigation. **Claudio Lovisolo:** Funding acquisition, Investigation, Writing – review & editing. **Maurizio Previati:** Conceptualization, Methodology. **Davide Canone:** Conceptualization, Data curation, Investigation, Methodology. **Stefano Ferraris:** Conceptualization, Data curation, Funding acquisition, Investigation, Project administration, Supervision, Validation, Writing – review & editing.

Declaration of competing interest

The authors declare that they have no known competing financial interests or personal relationships that could have appeared to influence the work reported in this paper.

Data availability

The dataset is available. The link is given in the manuscript

Acknowledgements

The authors would like to thank Prof. Jirka Simunek and his staff (University of California, Riverside) for providing the code of the Hydrus 1D model with the “double vegetation” modification. The authors also thank Dr. Stefano Bechis for the help in the field work and Prof. Alexander Knohl and Dr. Lukas Siebicke (University of Goettingen) for the valuable advice given during the development of the paper. The authors are grateful to the two anonymous reviewers for their valuable suggestions which improved the paper. The work was supported by Project NODES, which received funding from the MUR-M4C2 1.5 of the National Recovery and Resilience Plan (PNRR) with grant agreement no. ECS00000036, by Project PE9 GRINS Growing Resilient, Inclusive and Sustainable, financed by the Next Generation EU program (National Recovery and Resilience Plan) in the frame of the SPOKE 6 – WP1 activity, grant agreement no. PE0000018 - CUP D13C22002160001, by Project SUNSET, PRIN MUR 202295PFKP and by Project WATZON, PRIN MIUR 2017SL7ABC_005.

Data statement

The Cogne site database is published online at https://zenodo.org/records/10638628 (https://doi.org/10.5281/zenodo.10638627). A revised version, with added metadata, is available at https://zenodo.org/records/10891035 (https://doi.org/10.5281/zenodo-10891035). The software is available upon request to the corresponding author. The Hydrus 1D with double vegetation executable and its description are available upon request to either Prof. Jirka Simunek or the corresponding author with the consent of Prof. Jirka Simunek.

References

Ahlmann-Eltze, C., Patil, I., 2021. ggsignif: R Package for displaying significance brackets for ggplot2. PsyArxiv. https://doi.org/10.31234/osf.io/7awm6.

Allen, R., Pereira, L., Raes, D., Smith, M., 1998. FAO Irrigation and drainage paper No. 56. Rome: Food and Agriculture Organization of the United Nations 56, 26–40.

Archer, S.R., Andersen, E.M., Predick, K.I., Schwinning, S., Steidl, R.J., Woods, S.R., 2017. Woody Plant Encroachment: Causes and Consequences. In: Briske, D.D. (Ed.), Rangeland Systems: Processes, Management and Challenges, Springer Series on Environmental Management. Springer International Publishing, Cham, pp. 25–84. https://doi.org/10.1007/978-3-319-46709-2_2.

Baiamonte, G., Mercalli, L., Berro, D.C., Agnese, C., Ferraris, S., 2019. Modelling the frequency distribution of inter-arrival times from daily precipitation time-series in North-West Italy. Hydrol. Res. 50, 1. https://doi.org/10.2166/NH.2018.042.

Baur, P., Müller, P., Herzog, F., 2007. Alpweiden im Wandel. Agrarforschung 14, 254–259.

Ben Hamouda, G., Tomozeiu, R., Pavan, V., Antolini, G., Snyder, R.L., Ventura, F., 2021. Impacts of climate change and rising atmospheric CO2 on future projected reference evapotranspiration in Emilia-Romagna (Italy). Theor. Appl. Climatol. 146, 801–820. https://doi.org/10.1007/s00704-021-03745-3.

Berninger, F., Susiluoto, S., Gianelle, D., Bahn, M., Wohlfahrt, G., Sutton, M.A., Garcia-Pausas, J., Gimeno, C., Sanz, M.J., Dore, S., Rogiers, N., Furger, M., Eugster, W., Balzarolo, M., Sebastià, M.T., Tenhunen, J., Staszewski, T., Cernusca, A., 2015. Management and site effects on carbon balances of European mountain meadows and rangelands. Boreal Environ. Res. 20 (6), 748–760. https://helda.helsinki.fi/items/f2e90b03-bc2b-47ef-806c-a703c3aaaf5a.

Bertoldi, G., Della Chiesa, S., Notarnicola, C., Pasolli, L., Niedrist, G., Tappeiner, U., 2014. Estimation of soil moisture patterns in mountain grasslands by means of SAR RADARSAT2 images and hydrological modeling. J. Hydrol. 516, 245. https://doi.org/10.1016/j.jhydrol.2014.02.018.

Beven, K., 1993. Prophecy, reality and uncertainty in distributed hydrological modelling. Adv. Water Resour. 16 (1), 41–51. https://doi.org/10.1016/0309-1708(93)90028-E.

Beven, K., 2006. A manifesto for the equifinality thesis. J. Hydrol. 320 (1–2), 18–36. https://doi.org/10.1016/j.jhydrol.2005.07.007.
Bonan, G., 2015. Ecological Climatology: Concepts and Applications, 3rd ed. Cambridge University Press, Cambridge. https://doi.org/10.1017/CBO9781107339200.
Bonfils, C.J.W., Phillips, T.J., Lawrence, D.M., Cameron-Smith, P., Riley, W.J., Subin, Z. M., 2012. On the influence of shrub height and expaneion on nothern high latitude climate. Environ. Res. Lett. 7, 015503 https://doi.org/10.1088/1748-9326/7/1/015503.
Bottazzi, M., Bancheri, M., Mobilia, M., Bertoldi, G., Longobardi, A., Rigon, R., 2021. Comparing Evapotranspiration Estimates from the GEOframe-Prospero Model with Penman-Monteith and Priestley-Taylor Approaches under Different Climate Conditions. Water 13, 1221. https://doi.org/10.3390/w13091221.
Budyko, M.I., 1974. Climate and Life. Academic Press, New York, p. 507.
Calanca, P., Roesch, A., Jasper, K., Wild, M., 2006. Global warming and the summertime evapotranspiration regime of the Alpine region. Clim. Change 79, 65–78. https://doi.org/10.1007/s10584-006-9103-9.
Carrer, M., Pellizzari, E., Prendin, A.L., Pividori, M., Brunetti, M., 2019. Winter precipitation - not summer temperature - is still the main driver for Alpine shrub growth. Sci. Total Environ. 682, 171–179. https://doi.org/10.1016/j.scitotenv.2019.05.152.
Carrer, M., Dibona, R., Prendin, A.L., Brunetti, M., 2023. Recent waning snowpack in the Alps is unprecedented in the last six centuries. Nat. Clim. Chang. 13, 155–160. https://doi.org/10.1038/s41558-022-01575-3.
Caviezel, C., Hunziker, M., Schaffner, M., Kuhn, N.J., 2014. Soil–vegetation interaction on slopes with bush encroachment in the central Alps – adapting slope stability measurements to shifting process domains. Earth Surf. Proc. Land. 39, 509–521. https://doi.org/10.1002/esp.3513.
Caviezel, C., Hunziker, M., Kuhn, N.J., 2017. Green alder encroachment in the European Alps: The need for analyzing the spread of a native-invasive species across spatial data. Catena 159, 149–158. https://doi.org/10.1016/j.catena.2017.08.006.
Condon, L.E., Atchley, A.L., Maxwell, R.M., 2020. Evapotranspiration depletes groundwater under warming over the contiguous United States. Nat. Commun. 11, 873. https://doi.org/10.1038/s41467-020-14688-0.
D'Amico, M.E., Pintaldi, E., Sapino, E., Colombo, N., Quaglino, E., Stanchi, S., Navillod, E., Rocco, R., Freppaz, M., 2020. Soil types of Aosta Valley (NW-Italy). J. Maps 16 (2), 755–765. https://doi.org/10.1080/17445647.2020.1821803.
Dai, C., Wang, T., Zhou, Y., Deng, J., Li, Z., 2019. Hydraulic properties in different soil architectures of a small agricultural watershed: Implications for runoff generation. Water 11 (12), 2537. https://doi.org/10.3390/w11122537.
Della Chiesa, S., Bertoldi, G., Niedrist, G., Obojes, N., Endrizzi, S., Albertson, J.D., Wohlfahrt, G., Hoertnagl, L., Tappeiner, U., 2014. Modelling changes in grassland hydrological cycling along an elevational gradient in the Alps. Ecohydrology 7, 1453–1473. https://doi.org/10.1002/eco.1471.
Detsch, F., Otte, I., Appelhans, T., Nauss, T., 2017. A glimpse at short-term controls of evapotranspiration along the southern slopes of Kilimanjaro. Environ. Monit. Assess. 189, 465. https://doi.org/10.1007/s10661-017-6179-9.
Ding, L., Wang, P., Zhang, W., Zhang, Y., Li, S., Wei, X., Chen, X., Zhang, Y., Yang, F., 2020. Soil stoichiometry modulates effects of shrub encroachment on soil carbon concentration and stock in a subalpine grassland. iForest – Biogeosci. For. 13, 65. https://doi.org/10.3832/ifor3091-012.
Endrizzi, S., Gruber, S., Dall'Amico, M., Rigon, R., 2013. GEOtop: simulating the combined energy and water balance at and below the land surface accounting for soil freezing, snow cover and terrain effects. Geosci. Model Dev. Discuss. 6, 6279–6341. https://doi.org/10.5194/gmdd-6-6279-2013.
Feddes, R.A., Kowalik, P.J., Zaradny, H., 1978. Simulation of Field Water Use and Crop Yields. Simulation Monographs. University of Wageningen, 189 pp. ISBN 902200676X.
Filippa, G., Cremonese, E., Galvagno, M., Isabellon, M., Bayle, A., Choler, P., Carlson, B. Z., Gabellani, S., Morra di Cella, U., Migliavacca, M., 2019. Climatic drivers of greening trends in the Alps. Remote Sens. (Basel) 11, 2527. https://doi.org/10.3390/rs11212527.
Foken, T., 2008. Micrometeorology. Springer-Verlag, Berlin, Heidelberg, p. 306 pp..
Galvagno, M., Wohlfahrt, G., Cremonese, E., Filippa, G., Migliavacca, M., Morra di Cella, U., van Gorsel, E., 2017. Contribution of advection to nighttime ecosystem respiration at a mountain grassland in complex terrain. Agric. For. Meteorol. 237–238, 270–281. https://doi.org/10.1016/j.agrformet.2017.02.018.
Gentile, A., Canone, D., Ceperley, N., Gisolo, D., Previati, M., Zuecco, G., Schaefli, B., Ferraris, S., 2023. Towards a conceptualization of the hydrological processes behind changes of young water fraction with elevation: a focus on mountainous alpine catchments. Hydrol. Earth Syst. Sci. 27 (12), 2301–2323. https://doi.org/10.5194/hess-27-2301-2023.
Gisolo, D., Bevilacqua, I., van Ramshorst, J., Knohl, A., Siebicke, L., Previati, M., Canone, D., Ferraris, S., 2022. Evapotranspiration of an abandoned grassland in the Italian Alps: influence of local topography, intra- and inter-annual variability and environmental drivers. Atmos. 13, 977. https://doi.org/10.3390/atmos13060977.
Goulden, M.L., Bales, R.C., 2014. Mountain runoff vulnerability to increased evapotranspiration with vegetation expansion. Proc. Natl. Acad. Sci. 111, 14071–14075. https://doi.org/10.1073/pnas.1319316111.
Grossiord, C., Buckley, T.N., Cernusak, L.A., Novick, K.A., Poulter, B., Siegwolf, R.T.W., Sperry, J.S., McDowell, N.G., 2020. Plant responses to rising vapor pressure deficit. New Phytol. 226, 1550–1566. https://doi.org/10.1111/nph.16485.
Gu, S., Tang, Y., Cui, X., Du, M., Zhao, L., Li, Y., Xu, S., Zhou, H., Kato, T., Qi, P., Zhao, X., 2008. Characterizing evapotranspiration over a meadow ecosystem on the Qinghai-Tibetan Plateau. J. Geophys. Res. Atmos. 113 https://doi.org/10.1029/2007JD009173.
He, Y., De Wekker, S.F.J., Fuentes, J.D., Litvak, M., 2010. On the impact of shrub encroachment on microclimate conditions in the northern Chihuahuan desert. J. Geophys. Res. 115, D21120. https://doi.org/10.1029/2009JD013529.
Hunziker, M., Caviezel, C., Kuhn, N.J., 2017. Shrub encroachment by green alder on subalpine pastures: Changes in mineral soil organic carbon characteristics. Catena 157, 35–46. https://doi.org/10.1016/j.catena.2017.05.005.
Kendall, M.G., Stuart, A., 1967. The Advanced Theory of Statistics. Volume 2, Inference and Relationship. Charles Griffin & Co. Ltd, London, 690 pp.
Khatami, S., Peel, M.C., Peterson, T.J., Western, A.W., 2019. Equifinality and flux mapping: a new approach to model evaluation and process representation under uncertainty. Water Resour. Res. 55 (11), 8922–8941. https://doi.org/10.1029/2018WR023750.
Komac, B., Alados, C.L., Camarero, J.J., 2011. Influence of topography on the colonization of subalpine grasslands by the Thorny Cushion Dwarf Echinospartum horridum. Arct. Antarct. Alp. Res. 43, 601–611. https://doi.org/10.1657/1938-4246-43.4.601.
Komac, B., Kefi, S., Nuche, P., Escos, J., Alados, C.L., 2013. Modeling shrub encroachment in subalpine grasslands under different environmental and management scenarios. J. Environ. Manage. 121, 160–169. https://doi.org/10.1016/j.envman.2013.01.038.
Leitinger, G., Tasser, E., Newesely, C., Obojes, N., Tappeiner, U., 2010. Seasonal dynamics of surface runoff in mountain grassland ecosystems differing in land use. J. Hydrol. 385, 95–104. https://doi.org/10.1016/j.jhydrol.2010.02.006.
Leitinger, G., Ruggenthaler, R., Hammerle, A., Lavorel, S., Schirpke, U., Clement, J.-C., Lamarque, P., Obojes, N., Tappeiner, U., 2015. Impact of droughts on water provision in managed alpine grasslands in two climatically different regions of the Alps. Ecohydrology 8, 1600–1613. https://doi.org/10.1002/eco.1607.
Li, H., Ma, X., Lu, Y., Ren, R., Cui, B., Si, B., 2021a. Growing deep roots has opposing impacts on the transpiration of apple trees planted in subhumid loess region. Agric Water Manag 258, 107207. https://doi.org/10.1016/j.agwat.2021.107207.
Li, H., Zhang, F., Zhu, J., Guo, X., Li, Y., Lin, L., Zhang, L., Yang, Y., Li, Y., Cao, G., Zhou, H., Du, M., 2021b. Precipitation rather than evapotranspiration determines the warm-season water supply in an alpine shrub and an alpine meadow. Agric. For. Meteorol. 300, 108318 https://doi.org/10.1016/j.agrformet.2021.108318.
Maestre, F.T., Bowker, M.A., Puche, M.D., Hinojosa, M.B., Martínez, I., García-Palacios, P., Castillo, A.P., Soliveres, S., Luzuriaga, A.L., Sánchez, A.M., Carreira, J. A., Gallardo, A., Escudero, A., 2009. Shrub encroachment can reverse desertification in semi-arid Mediterranean grasslands. Ecol. Lett. 12, 930–941. https://doi.org/10.1111/j.1461-0248.2009.01352.x.
Marquardt, D.W., 1963. An algorithm for least-squares estimation of nonlinear parameters. J. Soc. Ind. Appl. Math. 11, 431–441.
Martre, P., Cochard, H., Durand, J.-L., 2001. Hydraulic architecture and water flow in growing grass tillers (Festuca arundinacea Schreb.). Plant Cell Environ. 24, 65–76. https://doi.org/10.1046/j.1365-3040.2001.00657.x.
Meyer, S., Leifeld, J., Bahn, M., Fuhrer, J., 2012. Free and protected soil organic carbon dynamics respond differently to abandonment of mountain grassland. Biogeosciences 9, 853–865. https://doi.org/10.5194/bg-9-853-2012.
Minacapilli, M., Agnese, C., Blanda, F., Cammalleri, C., Ciraolo, G., D'Urso, G., Iovino, M., Pumo, D., Provenzano, G., Rallo, G., 2009. Estimation of actual evapotranspiration of Mediterranean perennial crops by means of remote-sensing based surface energy balance models. Hydrol. Earth Syst. Sci. 13, 1061–1074. https://doi.org/10.5194/hess-13-1061-2009.
Newman, B.D., Wilcox, B.P., Archer, S.R., Breshears, D.D., Dahm, C.N., Duffy, C.J., McDowell, N.G., Phillips, F.M., Scanlon, B.R., Vivoni, E.R., 2006. Ecohydrology of water-limited environments: a scientific vision. Water Resour. Res. 42, W06302. https://doi.org/10.1029/2005WR004141.
Ochoa-Sánchez, A., Crespo, P., Carrillo-Rojas, G., Sucozhañay, A., Célleri, R., 2019. Actual evapotranspiration in the High Andean Grasslands: A comparison of measurement and estimation methods. Front. Earth Sci. 7 https://doi.org/10.3389/feart.2019.00055.
Palazzi, E., Mortarini, L., Terzago, S., von Hardenberg, J., 2019. Elevation-dependent warming in global climate model simulations at high spatial resolution. Clim. Dyn. 52, 2685–2702. https://doi.org/10.1007/s00382-018-4287-z.
Patono, D.L., Said-Pullicino, D., Eloi Alcatrão, L., Firbus, A., Ivaldi, G., Chitarra, W., Ferrandino, A., Ricauda Aimonino, D., Celi, L., Gambino, G., Perrone, I., Lovisolo, C., 2022. Photosynthetic recovery in drought-rehydrated grapevines is associated with high demand from the sinks, maximizing the fruit-oriented performance. Plant J. 112 (4), 1098–1111. https://doi.org/10.1111/tpj.16000.
Patono, D.L., Eloi Alcatrão, L., Dicembrini, E., Ivaldi, G., Ricauda Aimonino, D., Lovisolo, C., 2023. Technical advances for measurement of gas exchange at the whole plant level: Design solutions and prototype tests to carry out shoot and rootzone analyses in plants of different sizes. Plant Sci. 326, 111505. https://doi.org/10.1016/j.plantsci.2022.111505.
Peters, A., Durner, W., Iden, S.C., 2017. Modified Feddes type stress reduction function for modeling root water uptake: Accounting for limited aeration and low water potential. Agric Water Manag 185, 126–136. https://doi.org/10.1016/j.agwat.2017.02.010.
R Core Team, 2021. R: A Language and Environment for Statistical Computing. R Foundation for Statistical Computing, Vienna, Austria. url: https://www.R-project.org/.
Raffelli, G., Previati, M., Canone, D., Gisolo, D., Bevilacqua, I., Capello, G., Biddoccu, M., Cavallo, E., Deiana, R., Cassiani, G., Ferraris, S., 2017. Local- and plot-scale measurements of soil moisture: Time and spatially resolved field techniques in plain, hill and mountain sites. Water 9, 706. https://doi.org/10.3390/w9090706.

Rigon, R., Bertoldi, G., Over, T.M., 2006. GEOtop: a distributed hydrological model with coupled water and energy budgets. J. Hydrometeorol. 7 (3), 371:388. https://doi.org/10.1175/JHM497.1.

Sade, N., Gebremedhin, A., Moshelion, M., 2012. Risk-taking plants. Plant Signal Behav. 7 (7), 767–770. https://doi.org/10.4161/psb.20505.

Schaap, M.G., Leij, F.J., van Genuchten, M.T., 2001. ROSETTA: a computer program for estimating soil hydraulic parameters with hierarchical pedotransfer functions. J. Hydrol. 251, 163–176. https://doi.org/10.1016/S0022-1694(01)00466-8.

Schirpke, U., Kohler, M., Leitinger, G., Fontana, V., Tasser, E., Tappeiner, U., 2017. Future impacts of changing land-use and climate on ecosystem services of mountain grassland and their resilience. Ecosyst. Serv. 26 (A), 79–94. https://doi.org/10.1016/j.ecoser.2017.06.008.

Schreiner-McGraw, A.P., Vivoni, E.R., Ajami, H., Sala, O.E., Throop, H.L., Peters, D.P.C., 2020. Woody plant encroachment has a larger impact than climate change on dryland water budgets. Sci. Rep. 10, 8112. https://doi.org/10.1038/s41598-020-65094-x.

Simunek, J., van Genuchten, M. Th., Sejna M., 2012. Hydrus: model use, calibration and validation. American Society of Agricultural and Biological Engineers, ISSN 2151-0032, vol. 55(4), 1261–1274. https://doi.org/10.13031/2013.42239.

Simunek, J., Sejna, M., Saito, H., Sakai, M., van Genuchten, M.Th., 2013. The HYDRUS-1D software package for simulating the one-dimensional movement of water, heat, and multiple solutes in variably-saturated media. Version 4.17. Department of Environmental Sciences, University of California Riverside, Riverside, California, 308 pp.

Simunek, J., Wendroth, O., van Genuchten, M.T., 1998. Parameter estimation analysis of the evaporation method for determning soil hydraulic properties. J. Soil Sci. Soc. Am. 62, 894–905. https://doi.org/10.2136/sssaj1998.03615995006200040007x.

Tang, Y., Wu, X., Chen, Y., 2018. Sap flow characteristics and physiological adjustments of two dominant tree species in pure and mixed plantations in the semi-arid Loess Plateau of China. J. Arid. Land 10, 833–849. https://doi.org/10.1007/s40333-018-0027-9.

Tasser, E., Tappeiner, U., Cernusca, A., 2005. Ecological Effects of Land-use Changes in the European Alps. In: Huber, U.M., Bugmann, H.K.M., Reasoner, M.A. (Eds.), Global Change and Mountain Regions: an Overview of Current Knowledge, Advances in Global Change Research. Springer Netherlands, Dordrecht, pp. 409–420. https://doi.org/10.1007/1-4020-3508-X_41.

Turekhanova, R., 1995. Root system formation of *Hippophae Rhamnoides L.* (seabucktorn). Acta Phytogeogr. Suecica. 81, Uppsala. ISBN 91-7210-081-8.

van den Bergh, T., Körner, C., Hiltbrunner, E., 2018. Alnus shrub expansion increases evapotranspiration in the Swiss Alps. Regional Environ. Change 18, 1375–1385. https://doi.org/10.1007/s10113-017-1246-x.

Vivoni, E.R., Pérez-Ruiz, E.R., Scott, R.L., Naito, A.T., Archer, S.R., Biederman, J.A., Templeton, N.P., 2022. A micrometeorological flux perspective on brush management in a shrub-encroached Sonoran Desert grassland. Agric. For. Meteorol. 313, 108763 https://doi.org/10.1016/j.agrformet.2021.108763.

Wang, S., Fu, B.J., Gao, G.Y., Yao, X.L., Zhou, J., 2012. Soil moisture and evapotranspiration of different land cover types in the Loess Plateau, China. Hydrol. Earth Syst. Sci. 16, 2883–2892. https://doi.org/10.5194/hess-16-2883-2012.

Wang, P., Li, X.-Y., Wang, L., Wu, X., Hu, X., Fan, Y., Tong, Y., 2018. Divergent evapotranspiration partition dynamics between shrubs and grasses in a shrub-encroached steppe ecosystem. New Phytol. 219 (4), 1325–1337. https://doi.org/10.1111/nph.15237.

Wegehenkel, M., Beyrich, F., 2014. Modelling hourly evapotranspiration and soil water content at the grass-covered boundary-layer field site Falkenberg, Germany. Hydrol. Sci. J. 59, 376–394. https://doi.org/10.1080/02626667.2013.835488.

Wieser, G., Hammerle, A., Wohlfahrt, G., 2008. The Water Balance of Grassland Ecosystems in the Austrian Alps. Arct. Antarct. Alp. Res. 40, 439–445. https://doi.org/10.1657/1523-0430(07-039)[WIESER]2.0.CO;2.